Article

Not peer-reviewed version

Blood Plasma Small Non-Coding RNAs as Diagnostic Molecules of Progesterone Receptor-Negative Phenotype of Serous Ovarian Tumors

Angelika V. Timofeeva *, Ivan S. Fedorov, Alexandra V. Asaturova, Maya V. Sannikova, Anna V. Tregubova, Oleg A. Mayboroda, Grigory N. Khabas, Vladimir E. Frankevich, Gennady T. Sukhikh

Posted Date: 18 July 2023

doi: 10.20944/preprints202307.1155.v1

Keywords: miRNA; piRNA; mRNA; CA125; progesterone receptor (PGR); new-generation sequencing (NGS); quantitative RT-PCR; serous ovarian carcinoma; borderline cystadenoma; benign cystadenoma; formalin-fixed paraffin-embedded (FFPE) blocks; blood plasma; cytoreduction

Article

Blood Plasma Small Non-Coding RNAs as Diagnostic Molecules of Progesterone Receptor-Negative Phenotype of Serous Ovarian Tumors

Angelika V. Timofeeva [1,*], Ivan S. Fedorov [1], Aleksandra V. Asaturova [1], Maya V. Sannikova [1], Anna V. Tregubova [1], Oleg A. Mayboroda [2], Grigory N. Khabas [1], Vladimir E. Frankevich [1,3] and Gennady T. Sukhikh [1,4]

[1] National Medical Research Center for Obstetrics, Gynecology and Perinatology Named after Academician V.I. Kulakov Ministry of Healthcare of The Russian Federation, Ac. Oparina 4, 117997 Moscow, Russia
[2] Center for Proteomics and Metabolomics, Leiden University Medical Center, Postbus 9600, 2300 RC Leiden, The Netherlands
[3] Laboratory of Translational Medicine, Siberian State Medical University, 634050 Tomsk, Russia
[4] Department of Obstetrics, Gynecology, Perinatology and Reproductology, First Moscow State Medical University Named after I.M. Sechenov, 119991 Moscow, Russia
* Correspondence: v_timofeeva@oparina4.ru or avtimofeeva28@gmail.com; Tel.: +7-495-531-4444

Abstract: Progesterone receptor (PGR) expression level determines biological characteristics of the serous ovarian carcinoma, and low PGR expression appears to be associated with chemoresistance and worse outcome. In this study, we aimed to find relationships between tumor progesterone receptor level and RNA-profile (miRNAs, piwiRNAs, and mRNAs), determining its biological characteristics and behavior. For this purpose, we applied next generation sequencing of small noncoding RNAs, quantitative RT-PCR, and immunohistochemistry to analyze FFPE and frozen tumor samples as well as blood plasma from patients with benign cystadenoma (BSC), serous borderline tumour (SBT), low-grade and high-grade serous ovarian carcinoma (LGSOC and HGSOC, respectively). We found significant upregulation of MMP7 and MUC16 and downregulation of PGR in LGSOC and HGSOC in comparison with BSC. The tissue content of miR-199a-5p, miR-214-3p, miR-424-3p, miR-424-5p, miR-125b-5p significantly inversely correlated with the expression level of MUC16 and blood serum CA125 concentration, and significantly directly correlated with the PGR expression level in tumor tissue. On the contrary, the tissue content of miR-16-5p, miR-17-5p, miR-20a-5p, miR-93-5p, responsible for epithelial-mesenchymal transition (EMT) of the cell, significantly directly correlated with the blood serum CA125 concentration and significantly inversely correlated with the PGR expression level in the tumor tissue. Levels of the EMT-associated miRNAs significantly directly correlated with the content of hsa_piR_022437, hsa_piR_009295, hsa_piR_020813, hsa_piR_004307, hsa_piR_019914 in tumor tissues. Among them, expression level of hsa_piR_004307 significantly inversly correlated with the PGR expression level in the tumor. Two optimal logistic regression models were developed based on the quantitation of hsa_piR_020813, miR-16-5p, hsa_piR_022437 or hsa_piR_004307, hsa_piR_019914, miR-93-5p in the tumor tissue, both of which significantly diagnose PGR-negative tumor phenotype with 93% sensitivity. According to FunRich3.1.3 functional enrichment analysis tool, 72 gene-targets of miRNA and piRNA identified here as markers of PGR-negative ovarian tumor phenotype were proven to be mutated in different cancers such as ovarian, breast, colorectal, liver, stomach, lung, endometrial, thyroid cancer. Among them, the blood plasma levels of miR-16-5p and hsa_piR_022437 can be used to diagnose PGR-negative tumor phenotype with 86% sensitivity before surgery and chemotherapy to choose the treatment strategy for this most aggressive type of ovarian cancer (for instance, neoadjuvant chemotherapy followed by cytoreduction in combination with hyperthermic intraperitoneal chemotherapy) to increase the effectiveness of treatment and longevity of the patient.

Keywords: miRNA; piRNA; mRNA; CA125; progesterone receptor (PGR); new-generation sequencing (NGS); quantitative RT-PCR; serous ovarian carcinoma; borderline cystadenoma; benign cystadenoma; formalin-fixed paraffin-embedded (FFPE) blocks; blood plasma; cytoreduction

1. Introduction

According to world statistics, ovarian cancer ranks seventh in cancer mortality among women [1]. Despite ovarian cancer mortality has declined by more than 30% over the past 50 years due to improvements in treatment, survival rate is still fewer than 50% at 5 years after diagnosis [2]. The main methods of treatment of advanced ovarian cancer are a combination of surgery and chemotherapy (paclitaxel and platinum drugs in combination with bevacizumab or PARP inhibitors), the optimal order of which has not yet been determined. Cancer antigen 125 (CA125) is commonly used as a marker of ovarian cancer, but elevated levels are detected in only 50% of disease stage I and 80% of disease stage III-IV, and should be interpreted in conjunction with clinical signs and ultrasound findings due to nonspecificity and occurrence in other diseases [3–6]. It is used to monitor the patient's response to neo-adjuvant and adjuvant treatments [7,8], or to predict the overall survival probability at 3 months after the end of primary treatment: risk of death is 51% at 24 months and up to 79% at 60 months if a CA125 value is above 35 [9]. Significantly improvement diagnosis of early stage invasive serous ovarian/tubal carcinoma was the result of the two fully completed largest population clinical trials, using multimodal screening strategy (measurement serum level CA 125 and transvaginal ultrasound) [10,11]. But there was no significant reduction in ovarian cancer mortality compared to no screening cohort.

Different researcher teams are still elaborating new strategies ovarian cancer screening selecting biomarkers alone or in combination with CA 125, such as ROMA, CPH1, OVA1, Overa [12,13]. These approaches were developed to improve detecting early-stage disease aimed to reduce ovarian cancer mortality. But the aggressive behavior of a tumor is caused by its biological properties (extensive stromal reaction and increased invasiveness), which determine the failure of cytoreductive surgery, as well as chemoresistance [14]. Recent studies revealed that hormone receptor status defines tumor invasive properties and longevity, in particular, low levels of progesterone receptor (PGR) expression are associated with a more aggressive disease course and worse outcome in LGSOC and HGSOC [15,16], endometrioid carcinoma [17]. On the contrary, improved survival rate in patients with poorly differentiated epithelial ovarian tumors was associated with high serum progesterone in combination with expression of PGR [18]. The protective effect of progesterone may be due in part to PGR mediated suppression of progesterone receptor membrane component-1 providing the sensitivity of ovarian cancer cells to platinum-based chemotherapy [19].

The main regulators of signalling pathways in a cell through gene expression level control at the transcriptional and post-transcriptional levels are small non-coding RNAs, including microRNAs (miRNAs) and piwiRNA (piRNA). Changed profiles of many miRNAs, implicated in pathogenesis of the gynecological diseases, have been identified [20,21] and showed a clear histotype specific pattern [22]. Role of piRNAs in diverse kinds of cancers have been also demonstrated [23]. Recently, PIWI proteins and piRNAs play a prometastatic role in ovarian carcinoma, contributing to disease progression, and are considered as potential diagnostic and prognostic biomarkers for ovarian cancer [24,25].

Therefore, in the present study, it was of interest to find the relationship between the level of progesterone receptor expression in serous tumors and small non-coding RNAs, which are potential regulators of CA125 and epithelial-mesenchymal transition, forming an aggressive tumor phenotype and its chemoresistance. It was important to develop a noninvasive method of diagnosing progesterone receptor-negative tumor for the proper management of patients with this type of tumor.

2. Results

2.1. Analysis of tumor-specific miRNAs that regulate the level of CA125 in blood serum

In order to identify potential mechanisms of changes in CA125 secretion levels in patients with serous ovarian tumors, we compared miRNA sequencing data from tumor tissue (Table S1) and miRWalk data (http://mirwalk.umm.uni-heidelberg.de/). Comparison of the miRNA expression pattern in HGSOC tissue samples from patients P25, P26, P28 (Table 1) with benign cystadenoma tissue samples from patients P4, P6, P7 (Table 1) revealed 144 differentially expressed miRNAs (Table

Preprints (www.preprints.org) | NOT PEER-REVIEWED | Posted: 18 July 2023 doi:10.20944/preprints202307.1155.v1

S1, Sheet 1), among which 64 miRNAs were significantly downregulated (Table S1, Sheet 2). According to miRWalk, 31 of 64 miRNAs (Table S1, Sheet 3) are potential regulators of expression levels of mucin 16 (MUC16), matrix metalloproteinase 7 (MMP7) and matrix proteinase 9 (MMP9). At that, MMP7 and MMP9 presumably detach from MUC16 its extracellular domain, CA125 [26]. Moreover, increased expression/activity of MMP7 and MMP9 provides conditions for metastasis of ovarian cancer cells by remodeling the extracellular matrix and enhancing their migration and attachment to secondary sites [27]. In addition, MMP-7 upregulation can occur due to the interaction of the carboxy-terminal portion of the MUC16/CA125 protein and mesothelin causing an increase of invasive tumor properties [28,29]. The levels of the following miRNAs were analyzed in FFPE sections of tumor tissue from 38 patients (Table 1) by real-time quantitative PCR (Table S5): hsa-miR-199a-5p, hsa-miR-424-3p, hsa-miR-424-5p, hsa-miR-134-5p, hsa-miR-214-3p, hsa-miR-125b-5p, hsa-miR-139-5p.

The relative miRNA expression level was calculated from the difference between the threshold cDNA amplification cycles (Ct) of the analyzed miRNA and the reference endogenous SNORD68 (Figure 1). Analysis of the significance of differences in miRNA expression level (-ΔCt) in the compared groups was performed using a two-sided Wilcoxon-Mann-Whitney test (Table 2).

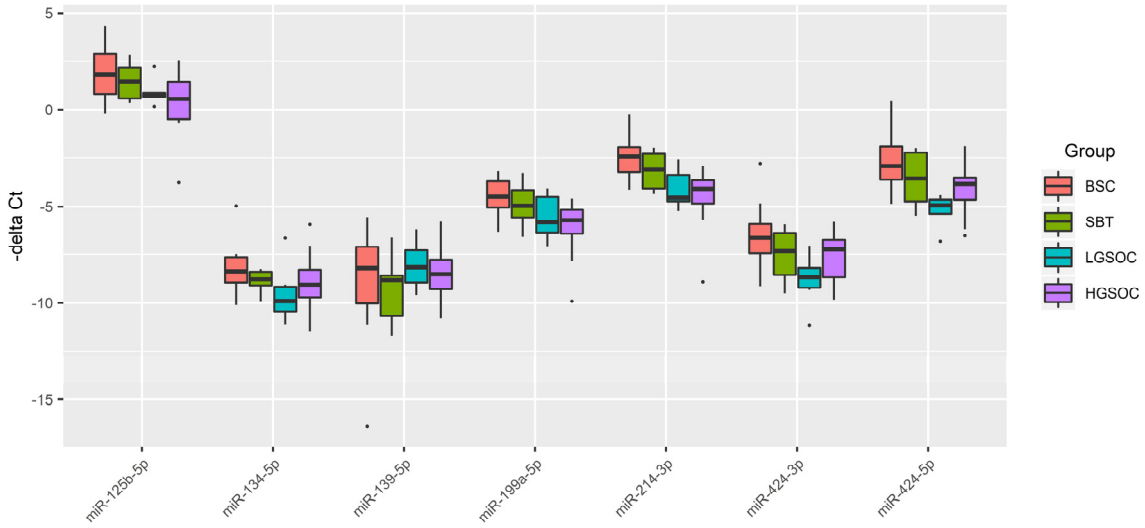

Figure 1. Box-plot of the expression level of miRNAs potentially regulating the level of CA-125 in serous ovarian tumors.

It follows from Figure 1 and Table 1 that in malignant ovarian neoplasms (SBT, LGSOC and HGSOC) the median expression level of analyzed miRNAs was lower than that in benign serous ovarian tumor (BSC), which is consistent with sequencing data (Table S1). A significant downregulation of miR-214-3p and miR-424-5p, potentially regulating MMP7 and/or MUC16, in the groups of serous ovarian carcinomas (LGSOC and HGSOC) was observed. Potential additional regulators of the expression level of MUC16 and MMP7 in the HGSOC group are miR-125b-5p and miR-199a-5p, whose expression level was significantly reduced relative to the BSC group. It should be noted that only the LGSOC group compared to the BSC group showed a significant decrease of miR-134-5p and miR-424-3p expression level, which potentially regulate the expression level of target genes MUC16 and MMP9. There were no significant differences between the SBT and the BSC groups in the expression levels of all analyzed miRNAs.

Table 1. Sample characteristics of the patients with serous ovary tumors.

Patient ID	Age, years	FIGO	1—primary tumor resection, 2—complete cytoreduction (size of residual tumor foci less than 2.5 mm), 3—suboptimal cytoreduction (size of residual tumor foci 2.5 mm - 2, 5 cm)	RECIST 1.1 MRI/CT criteria: 1-Complete Response, 2-Partial Response, 3-Stable Disease, 4-Progressive Disease	Diagnosis	ID, FFPE sample	progesterone receptor expression in tumor, Allred Score*	ID, blood plasma sample	CA 125 level before treatment, U/ml
P1	34	-	1	-	BSC	1	8	959	12
P2	41	-	1	-	BSC	7	8	724	18
P3	45	-	1	-	BSC	10	8	957	26
P4	53	-	1	-	BSC	17	8	802	12
P5	36	-	1	-	BSC	18	8	806	3
P6	46	-	1	-	BSC	24	8	866	3
P7	48	-	1	-	BSC	26	8	849	19
P8	43	-	1	-	BSC	31	8	908	11
P9	38	-	1	-	BSC	32	8	745	4
P10	45	-	1	-	BSC	37	8	705	9
P11	32	Ia	1	-	SBT	2	7	956	64
P12	35	Ia	1	-	SBT	22	8	453	15
P13	43	Ia	1	-	SBT	25	7	900	9
P14	36	Ia	1	-	SBT	27	7	510	55
P15	39	IB	1	-	SBT	33	7	817	12
P16	43	Ia	1	-	SBT	38	6	685	3
P17	34	IIIC	2	1	LGSOC	16	4	686	45
P18	54	IIIC	3	4	LGSOC	34	0	752	521
P19	46	IIIC	3	3	LGSOC	5	0	1004	41
P20	30	IIIC	3	3	LGSOC	6	0	554	604
P21	45	IIIC	2	1	LGSOC	8	4	731	173
P22	29	IIIC	2	4	LGSOC	15	5	796	550
P23	40	IIB	2	1	LGSOC	28	6	729	441
P24	53	IIIA	2	1	LGSOC	29	6	965	372
P25	63	IIIC	3	4	HGSOC	3	0	19	42

doi:10.20944/preprints202307.1155.v1

P26	51	IIIC	2	4	HGSOC	4	0	448	3808
P27	38	IIIC	3	4	HGSOC	9	0	2008	1244
P28	71	IIIC	3	4	HGSOC	11	0	13	517
P29	33	IIIC	3	2	HGSOC	12	6	939	59
P30	51	IIIC	2	3	HGSOC	13	0	679	2000
P31	45	IIB	2	3	HGSOC	14	0	782	517
P32	48	IC	2	4	HGSOC	19	0	11	190
P33	41	IIIC	2	1	HGSOC	20	3	672	1088
P34	54	IIIC	3	4	HGSOC	21	0	649	200
P35	42	IIIC	2	1	HGSOC	23	3	684	1293
P36	57	IIC	3	4	HGSOC	30	0	15	198
P37	77	IIIC	2	2	HGSOC	35	4	1060	1203
P38	45	IIA	2	3	HGSOC	36	0	22	60

* The Allred score combines the percentage of positive cells and the intensity of the reaction product in most of the carcinoma. Scores of 0-2 are considered negative. Scores of 3-8 are considered positive.

Table 2. Comparison of SBT, LGSOC and HGSOC groups relative to BSC by miRNA expression levels in serous ovarian tumors.

miRNA	Group	Me, -ΔCt	Q1	Q3	Wilcoxon-Mann-Whitney test, p-value	Potential gene-target
miR-125b-5p	BSC	1,79	0,83	2,91		MUC16, MMP7
	SBT	1,46	0,6	2,18	0,492258	
	LGSOC	0,79	0,68	0,89	0,101102	
	HGSOC	0,57	-0,49	1,45	0,022015	
miR-134-5p	BSC	-8,35	-8,95	-7,64		MUC16, MMP9
	SBT	-8,78	-9,1	-8,38	0,367632	
	LGSOC	-9,9	-10,45	-9,17	0,026647	
	HGSOC	-9,06	-9,71	-8,27	0,234983	
miR-139-5p	BSC	-8,19	-10,03	-7,12		MMP9
	SBT	-8,81	-10,7	-8,57	0,635365	
	LGSOC	-8,15	-8,94	-7,29	0,572604	
	HGSOC	-8,5	-9,3	-7,77	0,752095	
miR-199a-5p	BSC	-4,5	-5,05	-3,72		MUC16, MMP7
	SBT	-4,96	-5,58	-4,16	0,562188	
	LGSOC	-5,83	-6,35	-4,51	0,067599	

doi:10.20944/preprints202307.1155.v1

	HGSOC	-5,73	-6,41	-5,17	0,007251	
miR-214-3p	BSC	-2,43	-3,24	-1,93		MUC16, MMP7
	SBT	-3,1	-4,08	-2,29	0,263487	
	LGSOC	-4,55	-4,73	-3,38	0,006216	
	HGSOC	-4,09	-4,84	-3,67	0,000274	
miR-424-3p	BSC	-6,63	-7,45	-5,93		MUC16, MMP9
	SBT	-7,34	-8,54	-6,37	0,313187	
	LGSOC	-8,66	-9,23	-8,19	0,006216	
	HGSOC	-7,25	-8,67	-6,75	0,137503	
miR-424-5p	BSC	-2,91	-3,63	-1,89		MUC16
	SBT	-3,57	-4,74	-2,23	0,492258	
	LGSOC	-4,94	-5,39	-4,65	0,001371	
	HGSOC	-3,86	-4,65	-3,52	0,041717	

doi:10.20944/preprints202307.1155.v1

Preprints (www.preprints.org) | NOT PEER-REVIEWED | Posted: 18 July 2023 doi:10.20944/preprints202307.1155.v1

2.2. Analysis of MMP7, MMP9, MUC16, and PGR gene expression levels in the serous ovarian tumors

The level of expression of the MMP7, MMP9, MUC16 and PGR genes was analyzed in 38 samples of FFPE sections of serous tumors BSC, SBT, LGSOC, HGSOC (Table 1) by quantitative real-time PCR, using GAPDH, TUBA1B, ACTNB as reference genes (Figure 2, Tables 3 and S5). For MMP7, MMP9, and MUC16 mRNAs, there is a trend toward increased expression level, and for PGR mRNA – a trend toward decreased expression levels in malignant serous tumors (SBT, LGSOC, HGSOC) compared to benign serous tumors (BSC). A significant increase of MMP7, MMP9, and MUC16 gene expression levels was observed in the serous ovarian carcinoma groups (LGSOC and HGSOC) relative to the BSC group (Table 3). A statistically significant increase in the expression level of MMP7 and MUC16 was detected in the SBT group relative to the BSC group (Table 3). Multidirectional significant changes in the expression level of the MMP7 and MUC16 genes and their potential regulators miR-214-3p, miR-424-5p, miR-125b-5p and miR-199a-5p were revealed in the HGSOC group (Figures 1 and 2). In the LGSOC group, multidirectional significant changes in the expression level of the MMP7, MMP9, and MUC16 genes and their potential regulators miR-214-3p, miR-424-5p, miR-134-5p, and miR-424-3p were revealed. It is important to note that along with a significant increase in the expression level of MMP7, MMP9 and MUC16, there is a significant decrease in the expression level of PGR in the LGSOC and HGSOC samples (Figure 2), that may provide the invasive properties of the tumor and the ability to metastasize.

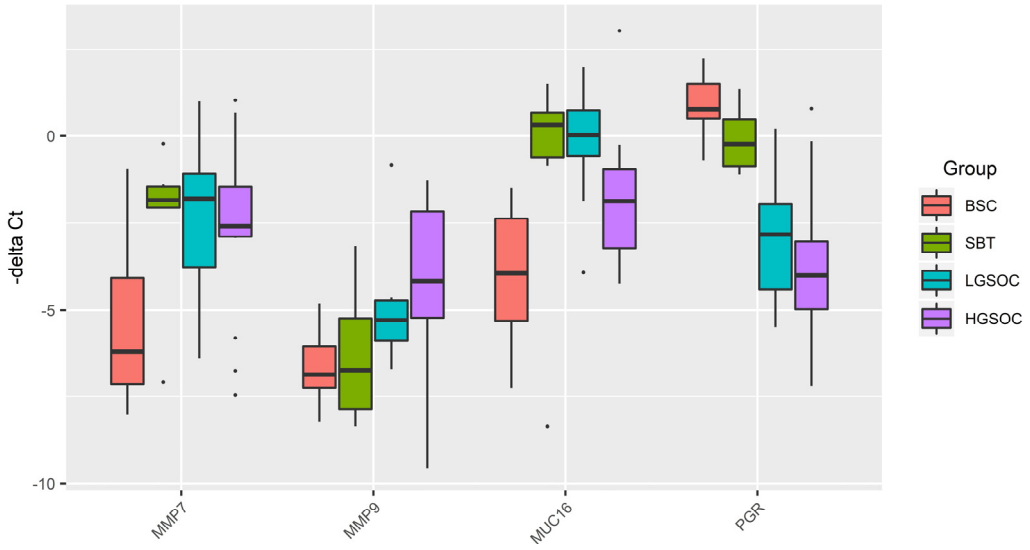

Figure 2. Box-plot of MMP7, MMP9, MUC16, and PGR mRNA expression level in serous ovarian tumors.

Preprints (www.preprints.org) | NOT PEER-REVIEWED | Posted: 18 July 2023 doi:10.20944/preprints202307.1155.v1

Table 3. Comparison of SBT, LGSOC and HGSOC relative to BSC by the mRNA expression level in serous ovarian tumors.

mRNA	Group	Me, -ΔCt	Q1	Q3	Wilcoxon-Mann-Whitney test, p-value
MMP7	BSC	-6,19	-7,14	-4,09	
	SBT	-1,84	-2,05	-1,45	0,041958
	LGSOC	-1,79	-3,78	-1,07	0,034279
	HGSOC	-2,59	-2,89	-1,45	0,030588
MMP9	BSC	-6,86	-7,24	-6,05	
	SBT	-6,74	-7,88	-5,23	0,874875
	LGSOC	-5,29	-5,89	-4,72	0,011655
	HGSOC	-4,18	-5,22	-2,16	0,022015
MUC16	BSC	-3,96	-5,3	-2,37	
	SBT	0,32	-0,61	0,68	0,031219
	LGSOC	0,03	-0,57	0,75	0,002057
	HGSOC	-1,86	-3,23	-0,94	0,018545
PGR	BSC	0,78	0,5	1,5	
	SBT	-0,23	-0,84	0,47	0,093407
	LGSOC	-2,83	-4,43	-1,95	0,000183
	HGSOC	-4,02	-4,97	-3,03	3,06E-05

2.3. Analysis of microRNA-regulators of EMT in the serous ovarian tumors tissue of

In a previous study [16], we detected differential expression of EMT-associated miR-16-5p, miR-17-5p, miR-20a-5p, miR-93-5p in the blood plasma of PGR-negative HGSOC patients. The present study aimed to analyze the expression level of these miRNAs in FFPE sections of serous tumors as a function of PGR expression level. The relative level of miRNA expression was calculated from the difference between the threshold cDNA amplification cycles of the analyzed miRNA and the reference endogenous SNORD68 (Figure 3).

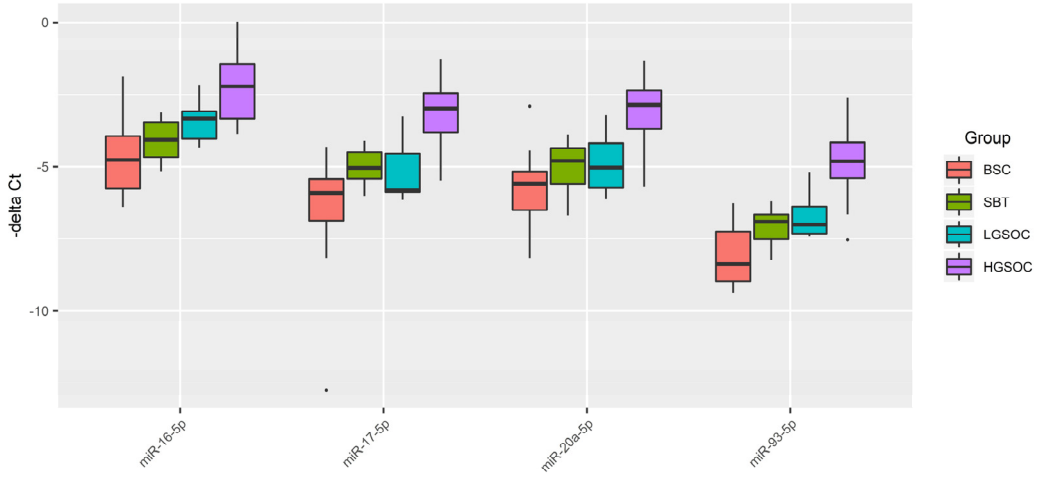

Figure 3. Box-plot of the expression level of miRNAs potentially regulating EMT in the serous ovarian tumors.

Figure 3 and Table 4 show that in malignant ovarian tumors (SBT, LGSOC and HGSOC) the median expression level of miRNAs that potentially regulate EMT was higher than that in benign serous ovarian tumors (BSC), which is consistent with miRNA sequencing data in tissues of serous tumors (Table S1, Sheet 1 and Sheet 4). A significant increase in the expression level of miR-16-5p, miR-17-5p, miR-20a-5p, and miR-93-5p was found in the HGSOC group relative to the BSC group,

Preprints (www.preprints.org) | NOT PEER-REVIEWED | Posted: 18 July 2023 doi:10.20944/preprints202307.1155.v1

which, along with a significant decrease in the PGR expression level and an increase in the expression level MMP7 and MUC16, potentially regulated by miR-214-3p, miR-424-5p, miR-125b-5p and miR-199a-5p with decreased levels, indicates a more aggressive behavior of the HGSOC in terms of the ability to metastasize compared to SBT and LGSOC. In the LGSOC group, a significant increase in miR-16-5p expression was found compared to BSC. In the SBT group, there were no significant changes in the analyzed miRNAs responsible for EMT.

Table 4. Comparative analysis of the expression level of miRNAs implicated in EMT in the SBT, LGSOC and HGSOC relative to BSC groups.

miRNA	Group	Me, -ΔCt	Q1	Q3	Wilcoxon-Mann-Whitney test, p-value
miR-16-5p	BSC	-4,76	-5,75	-3,94	
	SBT	-4,07	-4,65	-3,44	0,263487
	LGSOC	-3,32	-4,03	-3,07	0,034279
	HGSOC	-2,21	-3,32	-1,46	9,89E-05
miR-17-5p	BSC	-5,9	-6,86	-5,42	
	SBT	-5,04	-5,42	-4,49	0,072677
	LGSOC	-5,81	-5,86	-4,54	0,274281
	HGSOC	-2,97	-3,81	-2,45	3,06E-05
miR-20a-5p	BSC	-5,57	-6,51	-5,17	
	SBT	-4,79	-5,58	-4,34	0,313187
	LGSOC	-5,03	-5,72	-4,18	0,236985
	HGSOC	-2,86	-3,69	-2,36	0,000504
miR-93-5p	BSC	-8,37	-8,97	-7,23	
	SBT	-6,89	-7,51	-6,67	0,093407
	LGSOC	-7	-7,31	-6,38	0,067599
	HGSOC	-4,81	-5,4	-4,15	3,06E-05

2.4. Analysis of piRNA expression in serous ovarian tumors

One of the functions of piRNA is to regulate the stability of the cell genome by interacting in the nucleus with the retrotransposon transcript as part of the RISC complex, which contacts with histone deacetylase and histone methyltransferase and DNA methyltransferase, which block further transcription of the retrotransposon, thereby preventing its activity and integration into various genome regions [30]. In addition to the suppressive activity of piRNA against transposons, their regulatory effect on various signaling pathways in the cell is also known through both target mRNA destabilization/inhibition of translation and target mRNA stabilization/activation of translation [30] [31]. Due to proven genomic instability and changes in the activity of numerous signaling pathways in cancer cells, in particular, in serous ovarian carcinomas [15,32–36], we analyzed piRNA expression profiles in SBT tissue from patients P13, P15, P16 (Table 1) and in HGSOC tissue from patients P25, P26, P28 (Table 1) relative to that in BSC tissue from patients P4, P6, P7 (Table 1) by deep sequencing method (Table S2, Sheet 1 and Sheet 2). Ninety-seven piRNAs and 77 piRNAs differentially expressed in the HGSOC and SBT groups, respectively, were identified compared with BSC ($p < 0.1$), with the resulting lists of 37 piRNAs overlapping. For further analysis of 38 samples of FFPE tissue sections of serous ovarian tumors, 19 piRNAs were selected for quantitative real-time PCR (Table S5), six of which had an altered expression level in HGSOC and SBT, and the remaining 13 piRNAs – only in HGSOC. The relative level of piRNA expression was calculated from the difference between the threshold cycles of cDNA amplification of the analyzed piRNA and reference endogenous SNORD68 (Figure 4).

Preprints (www.preprints.org) | NOT PEER-REVIEWED | Posted: 18 July 2023 doi:10.20944/preprints202307.1155.v1

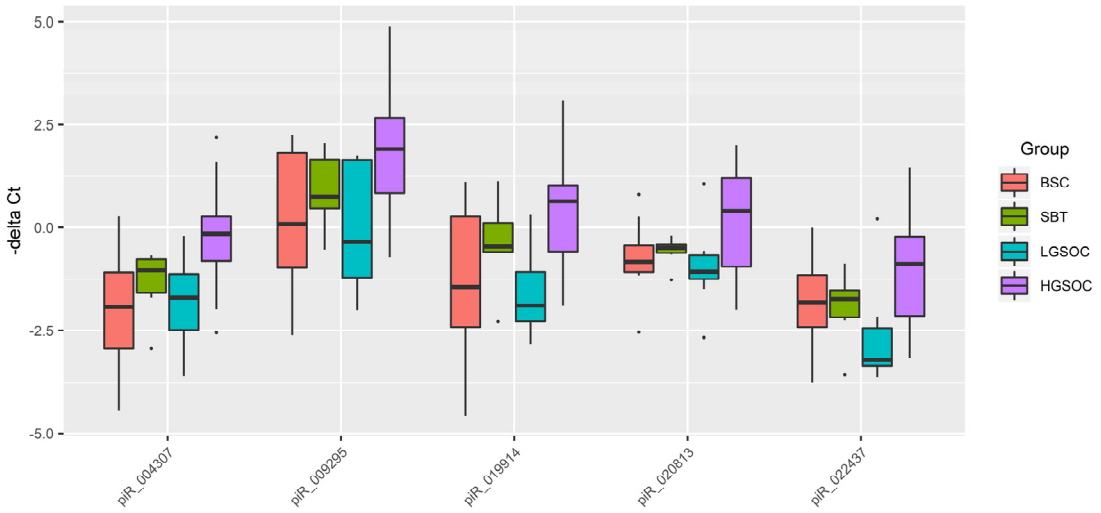

Figure 4. Box plot of piRNA expression level in FFPE sections of serous ovarian tumors.

Table 5. Comparative analysis of the piRNA expression level in the SBT, LGSOC and HGSOC relative to BSC groups in FFPE sections of tumor tissues.

piRNA	Group	Me, -ΔCt	Q1	Q3	Wilcoxon-Mann-Whitney test, p-value
hsa_piR_004307	BSC	-1,92	-2,92	-1,08	
	SBT	-1,03	-1,58	-0,75	0,21978
	LGSOC	-1,7	-2,49	-1,12	0,761826
	HGSOC	-0,14	-0,8	0,27	0,003067
hsa_piR_009295	BSC	0,09	-0,97	1,83	
	SBT	0,76	0,47	1,67	0,492258
	LGSOC	-0,33	-1,2	1,66	0,696467
	HGSOC	1,92	0,84	2,67	0,022015
hsa_piR_019914	BSC	-1,43	-2,41	0,27	
	SBT	-0,44	-0,57	0,12	0,427822
	LGSOC	-1,89	-2,28	-1,07	0,828557
	HGSOC	0,64	-0,57	1,04	0,015536
hsa_piR_020813	BSC	-0,82	-1,07	-0,42	
	SBT	-0,48	-0,6	-0,4	0,562188
	LGSOC	-1,06	-1,24	-0,66	0,359934
	HGSOC	0,41	-0,94	1,21	0,137503
hsa_piR_022437	BSC	-1,81	-2,42	-1,14	
	SBT	-1,73	-2,18	-1,51	1
	LGSOC	-3,2	-3,34	-2,44	0,083139
	HGSOC	-0,87	-2,14	-0,2	0,154081

Out of 19 piRNAs, a Ct value of less than 35 cycles was observed only in hsa_piR_004307, hsa_piR_009295, hsa_piR_019914, hsa_piR_020813, hsa_piR_022437, among which significant differences were found for hsa_piR_004307, hsa_piR_009295 and hsa_piR_019914 in the HGSOC group relative to BSC.

2.5. Correlation analysis of the expression level of tumor-associated miRNA, piRNA, mRNA, progesterone receptor and the level of CA125 in the blood serum of patients.

A Spearman correlation matrix was constructed to understand the potential relationships of the ovarian tumor process characteristics which form the molecular-biological portrait of serous tumors

Preprints (www.preprints.org) | NOT PEER-REVIEWED | Posted: 18 July 2023 doi:10.20944/preprints202307.1155.v1

of different types (Figure 5, Table S3). The analyzed samples were ranged, according to the diagnosis (type of the serous tumor) in the following way: "BSC" < "SBT" < "LGSOC" < "HGSOC". The expression level of hsa-miR-199a-5p, hsa-miR-214-3p, hsa-miR-424-5p, and hsa-miR-125b-5p were significantly inversely correlated with the expression level of MUC16 mRNA in the tumor tissue and with the CA125 level in the blood serum, but directly correlated with the level of PGR mRNA and PGR protein (according to Allred score). On the contrary, the expression level of miR-16-5p, miR-17-5p, miR-20a-5p, and miR-93-5p is significantly inversely correlated with the level of PGR, and directly correlated with the expression level of hsa_piR_004307, hsa_piR_009295, hsa_piR_019914, hsa_piR_020813, hsa_piR_022437 in the tumor tissue and with the CA125 level in the blood serum of patients. Among piRNAs, the hsa_piR_004307 expression level was significantly inversely correlated with the PGR protein level in the tumor tissue. MMP7 mRNA is significantly directly correlated with the level of MUC16 mRNA and MMP9 mRNA, which, in turn, is inversely correlated with the level of PGR. Note that the level of PGR mRNA is significantly correlated with the level of PGR protein, both of which are significantly inversely correlated with the level of CA125 in the blood serum of patients with serous ovarian tumors.

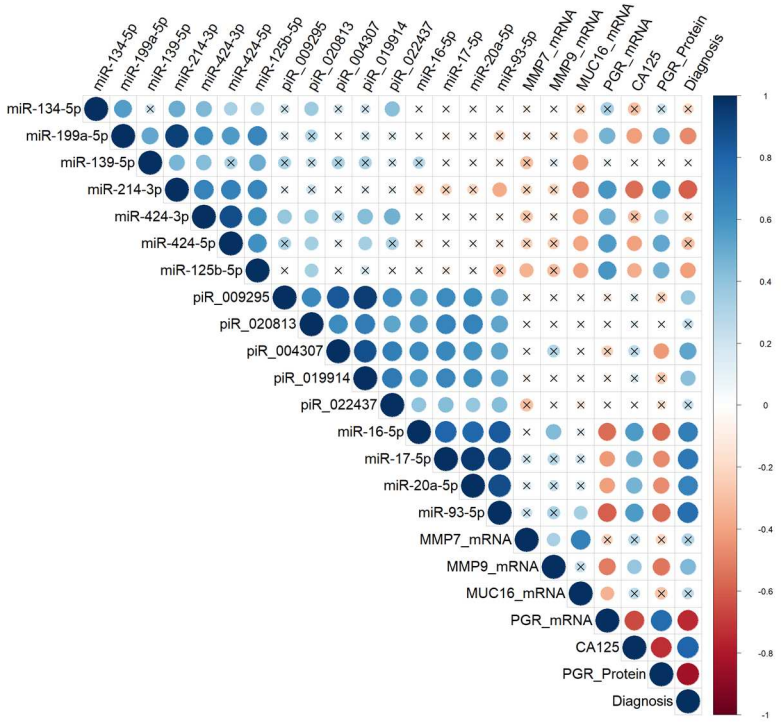

Figure 5. Correlation analysis of the miRNA, piRNA, mRNA expression levels, PGR protein level in 38 FFPE-samples of serous tumors and corresponding patient's blood serum CA125 level. Dot means significant correlations ($p < 0.05$), cross means non-significant correlations, among which direct correlations are highlighted in blue, and inverse correlations are highlighted in red. The larger the size of the dot, the more significant the correlation. The analyzed samples were ranged, according to the diagnosis (type of the serous tumor) in the following way: "BSC" < "SBT" < "LGSOC" < "HGSOC".

2.6. Partial least squares discriminant analysis (PLS-DA) of the molecular biological parameters determining certain type of tumor.

Since significant correlations were found between various molecular biological parameters depending on the type of serous ovarian tumor, it seemed interesting to evaluate the contribution of each parameter to the formation of a specific tumor type, namely: BSC, SBT, LGSOC, and HGSOC. All data obtained in sections 2.1 - 2.4 were used for partial least squares (PLS) analysis with the plotting the graph presented in Figure 6, which clearly shows the formation of clusters of samples depending on the type of serous tumor. The greatest contribution to the separation of BSC, SBT,

Preprints (www.preprints.org) | NOT PEER-REVIEWED | Posted: 18 July 2023 doi:10.20944/preprints202307.1155.v1

LGSOC, and HGSOC groups is made by molecules with VIP > 1: PGR expression level, miRNAs responsible for EMT (miR-16-5p, miR-17-5p, miR- 20a-5p, and miR-93-5p), hsa_piR_004307 (potential regulator of genome stability and signaling pathways in the cell), miR-214-3p (potential regulator of MMP7 and MUC16 expression levels), CA125 level in patients' blood serum, where the PGR expression level plays a primary role.

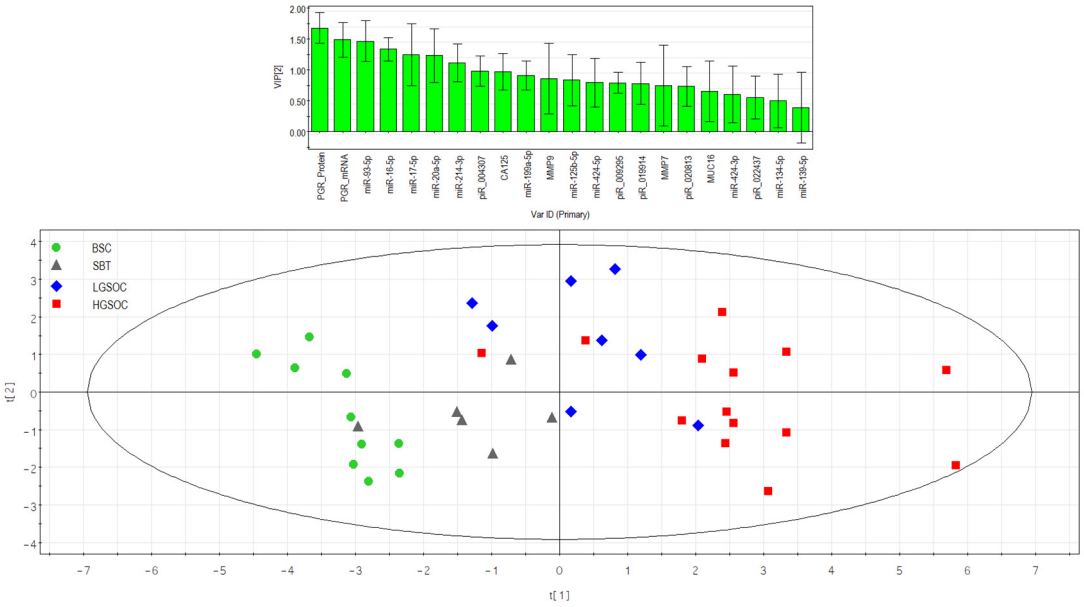

Figure 6. Partial least squares analysis (PLS) of "-ΔCt" RT-PCR data on the expression of miRNA, piRNA, mRNA, PGR protein in the 38 FFPE-samples of serous ovarian tumors and corresponding CA125 level in blood serum of patients. Score plot with the imposition of information of the molecular biological parameter value on the serous tumor type (BSC, SBT, LGSOC, and HGSOC) is presented in the bottom of the Figure. Variable Importance in Projection (VIP) score is presented at the top of the Figure.

2.7. Logistic regression models for diagnosing a progesterone receptor-negative serous ovarian tumor based on miRNA and piRNA expression levels in tumor tissue

The relationship between PGR expression level in tumor tissue and response to adjuvant chemotherapy was found, as shown in Table 1: in PGR-negative LGSOC and HGSOC, there was disease stabilization/progression in 75% and 100% cases, respectively. Due to the presence of correlations between the expression level of PGR and the expression level of small non-coding RNAs (miRNA and piRNA) as well as protein-coding mRNAs responsible for biological properties of a certain type of serous ovarian tumor, it was decided to develop a logistic regression model for tumor identification by PGR-phenotype. Based on the "-ΔCt" values obtained in Sections 2.1–2.4, logistic regression models were developed in RStudio program by finding the optimal combination of predictor variables with their stepwise inclusion and exclusion according to the contribution to the model and their significance, where the PGR expression level was dependent variable (0 - PGR-positive tumor, 1 - PGR-negative tumor in accordance with Allred score).

Table 6. Parameters of Figure 7 logistic regression models.

Coefficient	coefficient value (95% CI)	Wald test	p_value	Odds ratio (95% CI)	sensitivity	specificity
		model 1			0.7857	0.9167
(Intercept)	6.549(2.224;12.346)	2.618	0.008	698.816(9.245;230163.148)		
piR_020813	-1.504(-3.151;-0.316)	-2.144	0.032	0.222(0.042;0.728)		
piR_004307	1.142(0.198;2.475)	2.045	0.04	3.136(1.219;11.885)		
miR-93-5p	1.037(0.34;1.935)	2.614	0.008	2.823(1.405;6.928)		
		model 2			0.9286	0.7083

Preprints (www.preprints.org) | NOT PEER-REVIEWED | Posted: 18 July 2023 doi:10.20944/preprints202307.1155.v1

(Intercept)	6.701(2.428;13.488)	2.429	0.015	813.662(11.341;720717.037)		
piR_020813	-1.807(-3.818;-0.415)	-2.127	0.033	0.164(0.021;0.66)		
miR-16-5p	1.803(0.678;3.517)	2.56	0.01	6.073(1.97;33.695)		
piR_022437	1.248(0.259;2.713)	2.063	0.039	3.483(1.296;15.081)		
		model 3			0.9286	0.75
(Intercept)	6.803(2.115;13.645)	2.397	0.016	900.756(8.292;844027.632)		
piR_004307	2.748(0.756;5.757)	2.23	0.025	15.613(2.13;316.434)		
piR_019914	-2.168(-4.702;-0.446)	-2.046	0.04	0.114(0.009;0.639)		
miR-93-5p	0.881(0.209;1.811)	2.248	0.024	2.415(1.233;6.12)		
		model 4			0.8571	0.875
(Intercept)	4.319(1.219;8.825)	2.29	0.021	75.133(3.384;6806.095)		
piR_020813	-1.541(-3.308;-0.29)	-2.051	0.04	0.214(0.036;0.747)		
piR_004307	1.129(0.129;2.466)	1.951	0.051	3.093(1.138;11.782)		
miR-16-5p	1.327(0.374;2.65)	2.364	0.018	3.773(1.454;14.161)		
		model 5			0.8571	0.75
(Intercept)	7.585(2.542;14.208)	2.603	0.009	1969.531(12.709;1481859.036)		
piR_009295	-1.37(-2.869;-0.194)	-2.061	0.039	0.254(0.056;0.823)		
piR_004307	1.901(0.452;3.84)	2.276	0.022	6.698(1.572;46.542)		
miR-93-5p	0.772(0.174;1.53)	2.3	0.021	2.164(1.191;4.619)		
		model 6			0.7857	0.875
(Intercept)	6.903(2.61;12.621)	2.769	0.005	995.67(13.604;302894.002)		
piR_020813	-1.077(-2.305;-0.093)	-1.965	0.049	0.34(0.099;0.91)		
miR-93-5p	1.071(0.382;1.977)	2.697	0.006	2.92(1.466;7.221)		
piR_022437	0.72(0.006;1.611)	1.819	0.068	2.054(1.006;5.008)		

Models 2 and 3 in Figure 7 had the highest sensitivity (93%) in identifying PGR-negative tumors.

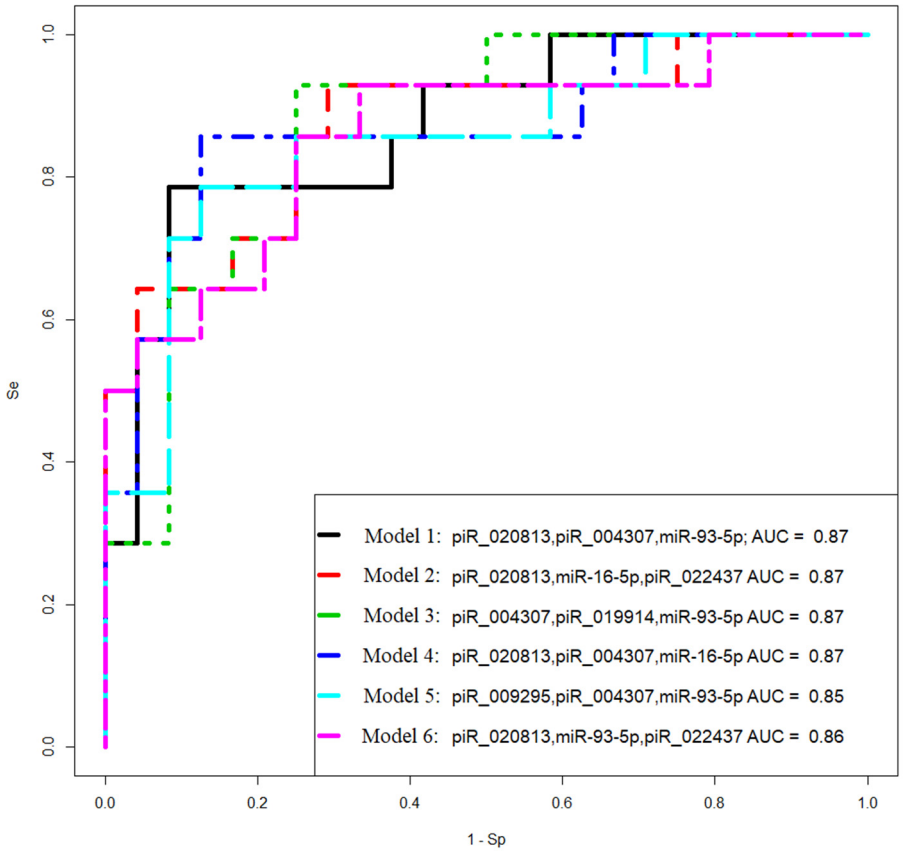

Figure 7. Receiver operating characteristic (ROC) curves of the logistic regression models to identify PGR-negative serous tumors based on the level of miRNA and piRNA in FFPE-samples of BSC, SBT, LGSOC, and HGSOC.

Preprints (www.preprints.org) | NOT PEER-REVIEWED | Posted: 18 July 2023 doi:10.20944/preprints202307.1155.v1

2.8. Logistic regression models for the diagnosis of progesterone receptor-negative serous ovarian tumor by the level of tumor-associated muıRNAs and piRNAs circulating in the blood of patients

To diagnose PGR-negative serous ovarian tumors before surgical and chemotherapeutic treatment, the content of miRNA and piRNA, forming models 2 and 3 of Figure 7, was analyzed by real-time RT-PCR in the blood plasma of 38 patients (ID number in Table 1). "-ΔCt" values were obtained when using hsa_piR_004308 as a reference molecule to quantify hsa_piR_020813, hsa_piR_022437, hsa_piR_004307, hsa_piR_019914, and when using hsa-miR-30d-5p as a reference molecule to analyze hsa-miR-16-5p and hsa-miR-93-5p levels. Logistic regression models were developed based on the obtained data and presented in Figure 8. Parameters of the developed models are presented in Table 7.

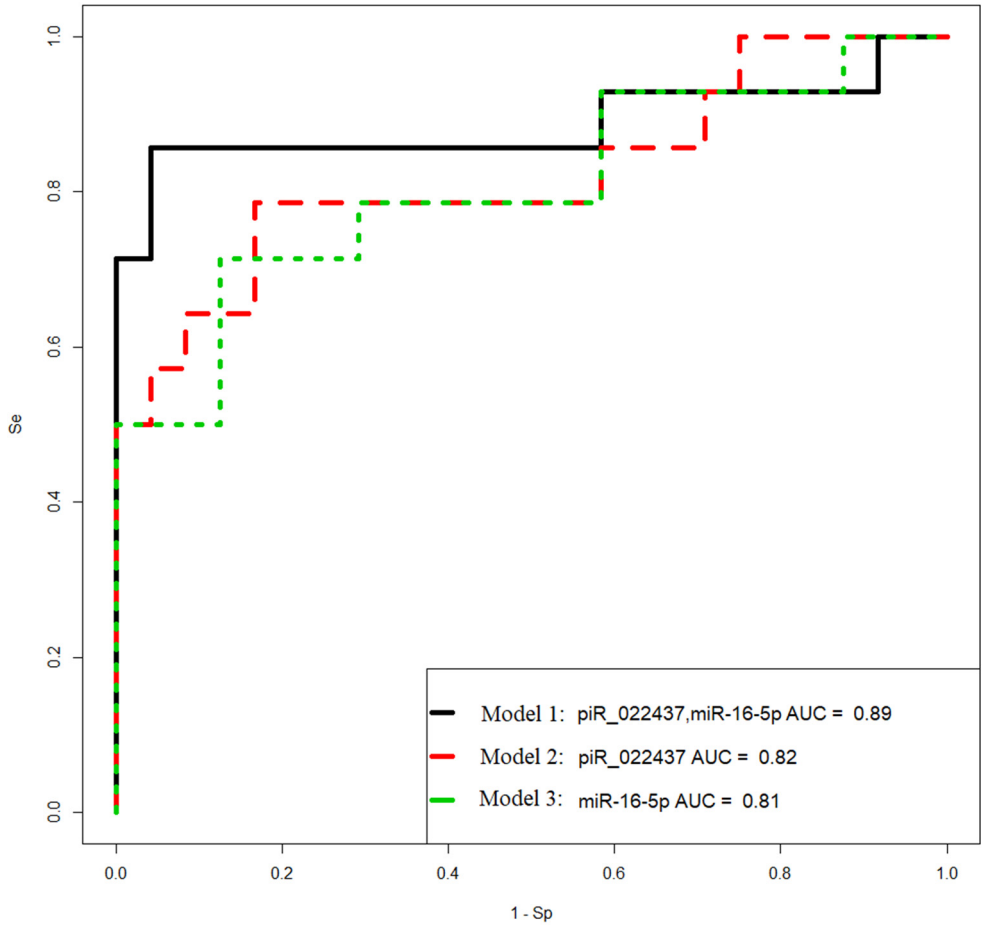

Figure 8. Receiver operating characteristic (ROC) curves of the logistic regression models to identify PGR-negative serous tumors based on the level of miRNA and piRNA in blood plasma samples from patients with BSC, SBT, LGSOC, and HGSOC.

Model 1 in Figure 8 has the highest sensitivity (86%) in identifying PGR-negative tumors. The formula describing this model is presented below:

$$\frac{1}{1 + e^{4.3 - 1.29x_1 - 0.75x_2}}$$

where x1 – "-ΔCt" for hsa_ piR_022437, x2 – "-ΔCt" for hsa_miR-16-5p.

Preprints (www.preprints.org) | NOT PEER-REVIEWED | Posted: 18 July 2023 doi:10.20944/preprints202307.1155.v1

Table 7. Parameters of Figure 8 logistic regression models.

Coefficient	coefficient value (95% CI)	Wald test	p_value	Odds ratio (95% CI)	sensitivity	specificity
		model 1			0.8571	0.9583
(Intercept)	-4.296(-7.698;-1.991)	-3.048	0.002	0.013(0.0004;0.136)		
piR_022437	1.288(0.399;2.683)	2.312	0.02	3.628(1.49;14.64)		
miR-16-5p	0.746(0.137;1.531)	2.173	0.029	2.109(1.147;4.625)		
		model 2			0.7857	0.8333
(Intercept)	-2.084(-3.604;-0.936)	-3.138	0.001	0.124(0.027;0.392)		
piR_022437	1.384(0.6;2.561)	2.861	0.004	3.991(1.822;12.957)		
		model 3			0.7143	0.875
(Intercept)	-3.326(-5.932;-1.428)	-2.956	0.003	0.035(0.002;0.239)		
miR-16-5p	0.921(0.36;1.671)	2.815	0.004	2.513(1.434;5.319)		

2.9. Functional Significance of RNA-markers associated with PGR-negative serous ovarian tumor phenotype

Potential targets of piRNAs from Figures 7 and 8 (piR_020813, piR_004307, piR_022437, piR_019914, piR_009295) were predicted as described in our recent manuscript [37]. The list of RNA targets for these piRNAs in the form of RefSeq mRNA accessions is presented in Table S4 (Sheet 1), followed by conversion to gene symbols using the bioDBnet database (https://biodbnet-abcc.ncifcrf.gov/db/db2db.php, last accessed on 15 March 2023). Potential target mRNAs for hsa-miR-16-5p and hsa-miR-93-5p were identified using miRtargetlink database (https://ccb-web.cs.uni-saarland.de/mirtargetlink/, last accessed on 15 March 2023). The total list of miRNA and piRNA gene-targets associated with the PGR-negative serous ovarian tumor phenotype is presented in Table S4 (Sheet 2). Functional significance of the target genes was assessed by the FunRich3.1.3 (http://www.funrich.org/download) functional enrichment analysis tool (Table, Sheet 3—Sheet 12). We found that among 3166 gene-targets for miRNA and piRNA from Figures 7 and 8 logistic regression models (Table S4, Sheet 2), 1421 genes are implicated in ovarian cancer (Table S4, Sheet8) and 101 genes that are involved in the pathogenesis of cancer when mutations occur in them according to the Cancer Gene Census from COSMIC database (Table S4, Sheet 11). These three gene lists were compared by Venny 2.1 (https://bioinfogp.cnb.csic.es/tools/venny/), the common one being a list of 72 genes (Figure 9A, Table S4, Sheet 12). Analysis of the expression site of 72 genes in the FunRich3.1.3 tool revealed experimentally proven involvement of these genes not only in ovarian cancer but also in breast, colorectal, liver, stomach, cervical, lung, endometrial, pancreatic, and thyroid cancers (Figure 9B).

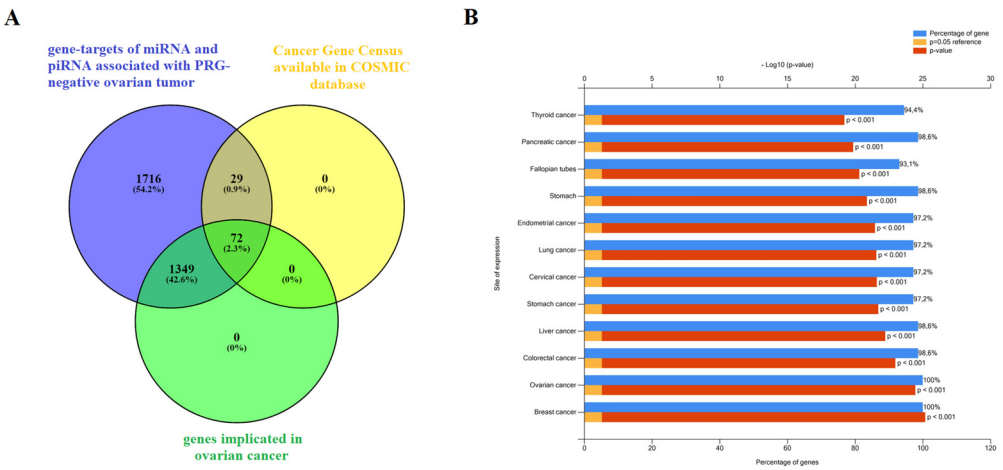

Figure 9. Functional significance of genes potentially regulated by miRNA and piRNA, associated with PGR-negative serous ovarian carcinoma phenotype. (**A**) Venn diagram of gene-targets for

 doi:10.20944/preprints202307.1155.v1

miRNA and piRNA from Figures 7 and 8 logistic regression models (Table S4, Sheet 2), genes, implicated in ovarian cancer according to FunRich3.1.3 (Table S4, Sheet 8), and genes, containing mutations that have been causally implicated in cancer according to the Cancer Gene Census from COSMIC database (Table S4, Sheet 11). (**B**) Site of expression of 72 genes, common for three gene lists as shown in (**A**), according to FunRich3.1.3 (Table S4, Sheet 12).

3. Discussion

Ovarian cancer is the most lethal gynecologic cancer with a 5-year survival rate of less than 50 percent [2]. The biological properties of the tumor (increased invasiveness, profound chromosomal instability in the cancer cells, and chemoresistance) dictated by the tumor microenvironment, especially cancer-associated fibroblasts, natural killer (NK) cells, Th2 cells [14,32,35,36]. It was revealed that hormone receptor status defines tumor invasive properties [15,18,38–40]. Increased expression levels of estrogen and progesterone receptors provides the better outcome for patients with ovarian cancer than reduced hormone receptors levels. In particular, aggressive form of the disease is characterized by low levels of PGR expression and worse outcome. Moreover, several polymorphisms in the hormone-binding domain in the PGR gene has been associated with increased risk of ovarian cancer [41–43]. The protective effect of progesterone may be due to PGR mediated suppression of progesterone receptor membrane component-1 (PGRMC1), increasing the sensitivity of ovarian cancer cells to platinum-based chemotherapy [19]. Thereby, targeted depletion of PGRMC1 could be used as an additional therapy to cisplatin. Recently, chemopreventive effect of synthetic progestin Norethindrone was demonstrated in epithelial ovarian cancer cells SKOV3 by upregulation of TP53 expression and downregulation of VEGF, HIF-1α, COX-2, and PGRMC1 expression, leading to significantly reduced SKOV3 cell growth, increased apoptosis and necrosis, and inhibiting cell migration [44]. The present study was aimed to explore and evaluate the candidate factors, namely miRNA, piRNA, mRNA, associated with the PGR-negative serous ovarian tumors, to develop a non-invasive test for identification this aggressive and chemoresistant tumor phenotype before any treatment and to and be prepared to use targeted therapies in addition to conventional treatment regimens.

We found a significant inverse correlation between the PGR expression level in ovarian tumor tissues and the CA125 serum level, which in turn significantly inversely correlated with the expression level of its potential regulators miR-199a-5p, miR-214-3p, miR-424-3p, miR-424-5p, miR-125b-5p, whose target genes are MUC16 and/or MMP7 and/or MMP9 according to miRWalk database. It was found that the downregulation of miR-199a-5p expression might be implicated in ovarian cancer progression in connection with the revealed negative correlation with tumor infiltration, tumor size, lymphatic metastasis and TNM stage in ovarian cancer [45]. Moreover, downregulated expression of miR-199a-5p was found in ascites-derived spheroids of the primary tumour site origin which form new metastatic niches due to high invasive capability [46]. Mir-214-3p has a suppressive effect on CDK6 [47] and on MAPK1 [48], and mir-214-3p downregulation facilitates the cell-cycle progression, proliferation, migration, and invasion of ovarian cancer cells. miR-424-3p has a proven capability to sensitize ovarian cancer cells to cisplatin by decreasing the expression of an anti-apoptotic protein galectin-3; in the case of galectin-3 overexpression, chemoresistance occurs [49]. In ovary cancer cells, miR-424/503 cluster is silenced by DNA hypermethylation, thereby canceling suppression of the expression of kinesin family member 23 by miR-424-5p and promoting cell proliferation and migration [50]. It is important to note that kinesins play an important regulatory role in the formation of spindles, separation of chromosomes, and cytokinesis, and in case of abnormal expression/function of kinesins, daughter cells become aneuploidic, thereby resulting in tumorigenesis [51]. In particular, elevated levels of KIF23 in ovarian, breast, lung cancer are associated with adverse outcomes [52–54]. miR-125b-5p may be considered as a platinum chemoresistance marker in connection with its strong downregulation in the tumorspheres originated from the SKOV-3 platinum-resistant cell line [55]. This relationship between chemoresistance and expression level of miR-125b-5p may be explained by direct targeting of BCL2 mRNA by miR-125b-5p thereby increasing the sensitivity of cancer cells to cisplatin treatment as it

 doi:10.20944/preprints202307.1155.v1

has been demonstrated for gallbladder cancer where low miR-125b-5p expression and high expression of Bcl2 was correlated with poor prognosis [56].

In the present study we found that MMP7 mRNA level was significantly directly correlated with the level of MUC16 mRNA and MMP9 mRNA, which, in turn, was inversely correlated with the level of PGR. We have found a direct correlation between the PGR and the miR-199a-5p, miR-214-3p, miR-424-3p, miR-424-5p, miR-125b-5p expression levels, and in the case of downregulation of these miRNAs in a PGR-negative serous tumor, the levels of MUC16, MMP7, and MMP9 can be increased, enhancing the ability of ovarian cancer cells to migrate, adhere to secondary sites and form metastasis [27], and providing tumor chemoresistance as discussed above. The maintenance of MMP7 concentration at a high level may be due to the induction of MMP-7 expression via a p38 mitogen-activated protein kinase (MAPK)-dependent pathwayas the result of the interaction of the carboxy-terminal portion of the MUC16/CA125 protein and mesothelin present on mesothelial cells lining the peritoneum [28,29]. Because high mesothelin correlates with chemoresistance and poor survival in epithelial ovarian carcinoma [57], several clinical trials are underway to evaluate the safety and efficacy of mesothelin-targeted drugs in platinum-resistant ovarian cancer [58,59].

In the present study, the tissue content of miR-16-5p, miR-17-5p, miR-20a-5p, miR-93-5p, responsible for epithelial-mesenchymal transition (EMT) of the cell [60–64], significantly directly correlated with the blood serum CA125 concentration and significantly inversely correlated with the PGR expression level in the tumor tissue. Found here increased levels of miR-20a-5p, miR-16-5p, miR-17-5p and miR-93-5p in tumor tissues and and peripheral blood from patients with HGSOC serous ovarian cancer are in good agreement with the literature data on the same direction of changes in the biological samples from patients with serous ovarian tumors [16,65–68]. It should be noted that a sharp significant decrease in the level of PGR mRNA was found in the present study in the LGSOC and HGSOC group, with a more pronounced drop in the case of the latter. This observation, along with a significant increase in the expression level of miR-20a-5p, miR-16-5p, miR-17-5p and miR-93-5p in the HGSOC group, probably indicates the most aggressive carcinoma phenotype among other types of serous tumors.

Levels of the EMT-associated miRNAs significantly directly correlated with the content of hsa_piR_022437, hsa_piR_009295, hsa_piR_020813, hsa_piR_004307, hsa_piR_019914 in serous ovarian tumor tissues. Among them, expression level of hsa_piR_004307 significantly inversly correlated with the PGR expression level in the tumor. One of the functions of piRNA is to regulate the stability of the cell genome by interacting in the nucleus with the retrotransposon transcript as part of the RISC complex, which contacts with histone deacetylase and methyltransferase, and DNA methyltransferase, which block further transcription of the retrotransposon, thereby preventing its activity and integration into different parts of the genome [30]. In addition to the suppressor activity of piRNAs against transposons, their regulatory effects on various signaling pathways in the cell through both destabilization of the target mRNA and inhibition of translation or stabilization of the target mRNA and activation of translation are also known to exist [30,31,69,70]. When analyzing potential target genes of hsa_piR_022437, hsa_piR_009295, hsa_piR_020813, hsa_piR_004307, hsa_piR_019914 and two miRNAs, miR-16-5p and miR-93-5p, involved in the identification of PGR-negative serous ovarian tumors by logistic regression method, the participation of 72 genes in pathogenesis of ovarian, breast, colorectal, liver, stomach, cervical, lung, endometrial, pancreatic, and thyroid cancers was proved, including the occurrence of mutations in these genes according to the Cancer Gene Census. Perhaps there are common pathogenetic mechanisms of epithelial cancers by altering the functional activity of this group of genes, in particular, under the action of miRNAs and piRNAs, used as prognostic parameters in developed logistic regression models.

The genome sequences, coding certain piRNA classes, are located within protein-coding genes, and functional piRNA molecules are mainly produced from the 3'-untranslated regions (3'-UTRs) of mRNA during their translation [71]. In addition, mRNAs 3'-UTR, producing piRNAs, usually contain transposon sequences whose activity is controlled by these piRNAs at the post-transcriptional level [72]. It is important to note that some piRNAs associated with the PGR-negative tumor phenotype are located in the loci of protein-coding genes and/or transposon, namely: the hsa_piR_022437 DNA

 doi:10.20944/preprints202307.1155.v1

sequence is related to retrotransposon SINE and located in the SUN1 gene involved in directed cell migration [73], and hsa_piR_009295 DNA sequence is located in the centrosome linker protein rootlein (encoding for CROCC gene with alternative name – TAX1BP2), whose overexpression inhibites centrosome duplication, whereas depletion results in centrosome hyperamplification [74] that is linked to oncogenesis [75,76]. Centrosome aberrations may induce the dissemination of metastatic cells and contribute to aggressive cancer subtypes [77].

After examining the tumor response to adjuvant chemotherapy, we found that in PGR-negative LGSOC and HGSOC, there was disease stabilization/progression in 75% and 100% cases, respectively. Thus, a substantial proportion of patients with primary PGR-negative LGSOC and HGSOC were resistant to platinum-based treatment that requires novel therapeutic and preventive approaches. In the present research, we developed non-invasive method based on regression analysis of hsa_piR_022437 *и* miR-16-5p content in the blood plasma from patients which can be used to diagnose PGR-negative tumor phenotype with 86% sensitivity before surgery and chemotherapy to choose the treatment strategy for this most aggressive type of ovarian cancer. Recently, a trial to investigate the effect of the addition of hyperthermic intraperitoneal chemotherapy (HIPEC) to interval cytoreductive surgery was conducted among patients with stage III epithelial ovarian cancer who were receiving neoadjuvant chemotherapy, and this procedure resulted in longer recurrence-free survival and overall survival than surgery alone [78]. It may be so that besides administration of HIPEC with cisplatin it is necessary to add targeted therapy aimed at depletion of PGRMC1, decreased mesothelin expression and Th2 infiltration to increase the effectiveness of treatment and longevity of the patient with highly aggressive serous ovarian tumor as PGR-negative type.

4. Materials and Methods

4.1. Patients enrolled in the study

38 women enrolled in the study aged between 29 and 71-years-old with primary ovarian tumors were referred to the National Medical Research Center for Obstetrics, Gynecology, and Perinatology, named after Academician V.I. Kulakov of the Ministry of Healthcare of the Russian Federation for clinical and instrumental additional examination and surgical intervention in the volume depending on the stage of the disease, which was histologically verified according to FIGO. After adjuvant chemotherapy (carboplatin AUC 6 + paclitaxel 175 mg/m2), tumor response was evaluated according to the RECIST 1.1 criteria. The following groups were formed: benign serous cystadenoma, n = 10; borderline serous cystadenoma, n = 6; low-grade serous ovary cancer, n = 8; high-grade serous ovary cancer, n = 14.

4.2. RNA Isolation from Peripheral Blood Plasma

S-MONOVETTE tubes containing EDTA KE (Sarstedt AG&Co., Ltd., Nümbrecht, Germany, cat. No. 04.1915.100) were used to sample venous blood from patients entrolled in the study. 200 μL of blood plasma collected after two-step centrifugation for 20 min at 300× g (4 °C) and for 10 min at 16,000× g, were used for RNA extraction applying an miRNeasy Serum/Plasma Kit (Qiagen, Germany, cat. No. 217184).

4.3. RNA isolation from ovarian tumors

Ovarian tumor samples were collected during surgery and immediately frozen in liquid nitrogen or embedded in paraffin blocks after fixation with neutral formalin, for subsequent total RNA extraction in the former case using the miRNeasy Micro Kit (Qiagen, Hilden, Germany, catalog No. 217084), followed by the RNeasy MinElute Cleanup Kit (Qiagen, Germany, catalog No. 74204) or in the latter case using deparaffinization solution (Qiagen, Hilden, Germany, catalog No.19093) and RNeasy FFPE Kit (Qiagen, Hilden, Germany, catalog No. 73504). Qubit fluorometer 3.0 (Life Technologies, Petaling Jaya, Malaysia, cat.Q33216) was used for RNA concentration measurement. Total RNA quality was examined on the Agilent Bioanalyzer 2100 (Agilent, Waldbronn, Germany,

 doi:10.20944/preprints202307.1155.v1

cat. No G2939A) using the RNA 6000 Nano Kit (Agilent Technologies, Santa Clara, CA, USA, cat. No. 5067-1511).

4.4. Small RNA Deep Sequencing

500 ng of total RNA from frozen tumor tissues were used for cDNA libraries synthesis applying the NEBNext® Multiplex Small RNA Library Prep Set for Illumina® (Set11 and Set2, New England Biolab®, Frankfurt am Main, Germany, cat. No. E7300S, E7580S). After amplification for 14 PCR cycles and purification in the 6% polyacrylamide gel, cDNA libraries were sequenced on the NextSeq 500 platform (Illumina, San Diego, AC, USA, cat. No. SY-415-1001). Deep sequencing data were processed as described in our previous publication [37], using Cutadapt to remove adapters, bowtie aligner [79] to map all trimmed reads in the range of 16 bp - 50 bp to the GRCh38.p15 human genomes, miRBase v21, and piRNABase, featureCount tool from the Subread package [80] to count aligned reads, and the DESeq2 package [81] to carry out differential expression analysis of the sncRNA.

4.5. Reverse Transcription and Quantitative Real-Time PCR of small noncoding RNA

Seven microliters of total RNA obtained in 4.2. or 250 ng of total RNA from FFPE samples obtained in 4.3. were converted into cDNA in accordance with the miScript® II RT Kit protocol (Qiagen, Germany, cat. No. 218161). After completion of the reaction and dilution of the sample by 20 times, cDNA (2 µL) was amplified during real-time PCR using a forward primer specific for the studied RNA (Table S5) and the miScript SYBR Green PCR Kit (Qiagen, Germany, cat. No. 218075). The following PCR conditions for miRNA and piRNA amplification were used: (1) 15 min at 95 °C and (2) 40 cycles at 94 °C for 15 s, an optimized annealing temperature (46.2–62 °C) for 30 s and 70 °C at 30 s in a StepOnePlusTM thermocycler (Applied Biosystems, Waltham, MA, USA, cat. No. 4376600). miR-30d-5p was used as the reference RNA to quantify miRNA and hsa_piR_004308 was used as the reference RNA to quantify piRNA in the blood plasma sample by the ΔCt method. The relative expression of miRNA and piRNA in the FFPE ovarian tumor sections was determined by the ΔCt method using SNORD68 as the reference RNA.

4.6. Reverse Transcription and Quantitative Real-Time PCR of mRNA

125 ng of total RNA from FFPE ovarian tumor sections, were converted into cDNA in a reaction mixture (25 µL) containing 10 µM random hexameric primer (Evrogen, Russia), 1x M-MLV RT buffer (M531A, Promega), 1x dNTP mix (0.2 mM each, Evrogen, Russia), 200 U M-MLV reverse transcriptase (M1708, Promega) at 37 °C over 60 min, followed by incubation at 95 °C over 10 min; then, the sample volume was adjusted with deionized water to 100 µL. The synthesized cDNA (2 µL) was used as a template for real-time PCR in a reaction mixture (20 µL) containing 150 nM each of the forward and reverse primers specific for the studied mRNA (Table S5) in a 1x qPCRmix-HS SYBR+HighROX (Evrogen, Russia). The following PCR conditions were used: (1) 5 min at 95 °C and (2) 40 cycles at 95 °C for 20 s, an optimized annealing temperature (48.9 – 63.8 °C) for 20 s and 72 °C at 30 s in a CFX96 Real-Time System (C1000 Touch Thermal Cycler plus CFX96 Optics Module, BioRad, Singapore). The relative expression of mRNA was determined by the ΔCt method using geometric mean of ACTB, TUBA, GAPDH as the reference RNAs.

4.7. Immunohistochemistry

PGR immunohistochemical staining of formalin-fixed paraffin-embedded specimens of serous ovarian tumors was performed as described in our previous publication [16] according to the Allred scale [82].

4.8. Statistical Analysis of the Obtained Data

Scripts written in R language [80] and RStudio [83] were used for statistical processing as described in our previous publication [16] applying Shapiro–Wilk test, the Mann–Whitney test for

paired comparison, Spearman's nonparametric correlation test, logistic regression analysis. Study results were considered reliable if the value of statistical significance (p) was less than 0.05.

Supplementary Materials: Table S1: miRNA deep sequencing data for serous ovarian tumors; Table S2: piRNA deep sequencing data for serous ovarian tumors; Table S3: Spearman's nonparametric correlation test data; Table S4: functional analysis of gene-targets for piRNAs and miRNAs from Figures 7 and 8; Table S5: parameters of PCR primers used to analyze miRNA, piRNA and mRNA.

Author Contributions: Conceptualization, A.V.Ti., I.S.F and O.A.M.; methodology, A.V.Ti., I.S.F., A.V.A, and A.V.Tr.; software, I.S.F., validation, A.V.Ti., I.S.F. and A.V.A; investigation, A.V.Ti., I.S.F., A.V.A, and A.V.Tr; resources, G.N.K. and A.V.A.; data curation, M.V.S. and G.N.K.; writing—original draft preparation, A.V.Ti..; writing—review and editing, I.S.F.; visualization, I.S.F; supervision, G.T.S.; project administration, V.E.F.; funding acquisition, V.E.F. All authors have read and agreed to the published version of the manuscript.

Funding: This study was supported by the Ministry of Science and Higher Education of the Russian Federation «Genetic and epigenetic editing of tumor cells and microenvironment in order to block metastasis» (agreement № 075-15-2021-1073)

Institutional Review Board Statement: All patients signed an informed consent to participate in the study, approved by the Ethics Committee of the NMRC for OGP (Protocol No. 10 of 05 December 2019). We confirm that the study was conducted in accordance with the ethical standards of the institutional research committee, the Federal Laws of the Russian Federation (No 152, 323, 1,130 etc.,) and with the 1964 Helsinki Declaration.

Informed Consent Statement: Informed consent was obtained from all subjects involved in the study.

Data Availability Statement: Not applicable.

Conflicts of Interest: The authors declare no conflict of interest.

References

1. Doherty, J.A.; Peres, L.C.; Wang, C.; Way, G.P.; Greene, C.S.; Schildkraut, J.M. Challenges and Opportunities in Studying the Epidemiology of Ovarian Cancer Subtypes. *Curr. Epidemiol. reports* **2017**, *4*, 211–220, doi:10.1007/s40471-017-0115-y.
2. Torre, L.A.; Trabert, B.; DeSantis, C.E.; Miller, K.D.; Samimi, G.; Runowicz, C.D.; Gaudet, M.M.; Jemal, A.; Siegel, R.L. Ovarian cancer statistics, 2018. *CA. Cancer J. Clin.* **2018**, *68*, 284–296, doi:10.3322/caac.21456.
3. Sturgeon, C.M.; Duffy, M.J.; Stenman, U.-H.; Lilja, H.; Brünner, N.; Chan, D.W.; Babaian, R.; Bast, R.C.J.; Dowell, B.; Esteva, F.J.; et al. National Academy of Clinical Biochemistry laboratory medicine practice guidelines for use of tumor markers in testicular, prostate, colorectal, breast, and ovarian cancers. *Clin. Chem.* **2008**, *54*, e11-79, doi:10.1373/clinchem.2008.105601.
4. Charkhchi, P.; Cybulski, C.; Gronwald, J.; Wong, F.O.; Narod, S.A.; Akbari, M.R. CA125 and Ovarian Cancer: A Comprehensive Review. *Cancers (Basel).* **2020**, *12*, 3730, doi:10.3390/cancers12123730.
5. Einhorn, N.; Sjövall, K.; Knapp, R.C.; Hall, P.; Scully, R.E.; Bast, R.C.J.; Zurawski, V.R.J. Prospective evaluation of serum CA 125 levels for early detection of ovarian cancer. *Obstet. Gynecol.* **1992**, *80*, 14–18.
6. Zhang, M.; Cheng, S.; Jin, Y.; Zhao, Y.; Wang, Y. Roles of CA125 in diagnosis, prediction, and oncogenesis of ovarian cancer. *Biochim. Biophys. acta. Rev. cancer* **2021**, *1875*, 188503, doi:10.1016/j.bbcan.2021.188503.
7. You, B.; Freyer, G.; Gonzalez-Martin, A.; Lheureux, S.; McNeish, I.; Penson, R.T.; Pignata, S.; Pujade-Lauraine, E. The role of the tumor primary chemosensitivity relative to the success of the medical-surgical management in patients with advanced ovarian carcinomas. *Cancer Treat. Rev.* **2021**, *100*, 102294, doi:10.1016/j.ctrv.2021.102294.
8. Lauby, A.; Colomban, O.; Corbaux, P.; Peron, J.; Van Wagensveld, L.; Gertych, W.; Bakrin, N.; Descargues, P.; Lopez, J.; Kepenekian, V.; et al. The Increasing Prognostic and Predictive Roles of the Tumor Primary Chemosensitivity Assessed by CA-125 Elimination Rate Constant K (KELIM) in Ovarian Cancer: A Narrative Review. *Cancers (Basel).* **2021**, *14*, doi:10.3390/cancers14010098.
9. Karamouza, E.; Glasspool, R.M.; Kelly, C.; Lewsley, L.-A.; Carty, K.; Kristensen, G.B.; Ethier, J.-L.; Kagimura, T.; Yanaihara, N.; Cecere, S.C.; et al. CA-125 Early Dynamics to Predict Overall Survival in Women with Newly Diagnosed Advanced Ovarian Cancer Based on Meta-Analysis Data. *Cancers (Basel).* **2023**, *15*, doi:10.3390/cancers15061823.
10. Menon, U.; Gentry-Maharaj, A.; Burnell, M.; Singh, N.; Ryan, A.; Karpinskyj, C.; Carlino, G.; Taylor, J.; Massingham, S.K.; Raikou, M.; et al. Ovarian cancer population screening and mortality after long-term

follow-up in the UK Collaborative Trial of Ovarian Cancer Screening (UKCTOCS): a randomised controlled trial. *Lancet (London, England)* **2021**, *397*, 2182–2193, doi:10.1016/S0140-6736(21)00731-5.

11. Buys, S.S.; Partridge, E.; Black, A.; Johnson, C.C.; Lamerato, L.; Isaacs, C.; Reding, D.J.; Greenlee, R.T.; Yokochi, L.A.; Kessel, B.; et al. Effect of screening on ovarian cancer mortality: the Prostate, Lung, Colorectal and Ovarian (PLCO) Cancer Screening Randomized Controlled Trial. *JAMA* **2011**, *305*, 2295–2303, doi:10.1001/jama.2011.766.
12. Liberto, J.M.; Chen, S.-Y.; Shih, I.-M.; Wang, T.-H.; Wang, T.-L.; Pisanic, T.R. 2nd Current and Emerging Methods for Ovarian Cancer Screening and Diagnostics: A Comprehensive Review. *Cancers (Basel).* **2022**, *14*, doi:10.3390/cancers14122885.
13. Giampaolino, P.; Foreste, V.; Della Corte, L.; Di Filippo, C.; Iorio, G.; Bifulco, G. Role of biomarkers for early detection of ovarian cancer recurrence. *Gland Surg.* **2020**, *9*, 1102–1111, doi:10.21037/gs-20-544.
14. Liu, Z.; Beach, J.A.; Agadjanian, H.; Jia, D.; Aspuria, P.-J.; Karlan, B.Y.; Orsulic, S. Suboptimal cytoreduction in ovarian carcinoma is associated with molecular pathways characteristic of increased stromal activation. *Gynecol. Oncol.* **2015**, *139*, 394–400, doi:10.1016/j.ygyno.2015.08.026.
15. Cheasley, D.; Fernandez, M.L.; Köbel, M.; Kim, H.; Dawson, A.; Hoenisch, J.; Bittner, M.; Chiu, D.S.; Talhouk, A.; Gilks, C.B.; et al. Molecular characterization of low-grade serous ovarian carcinoma identifies genomic aberrations according to hormone receptor expression. *NPJ Precis. Oncol.* **2022**, *6*, 47, doi:10.1038/s41698-022-00288-2.
16. Timofeeva, A. V; Asaturova, A. V; Sannikova, M. V; Khabas, G.N.; Chagovets, V. V; Fedorov, I.S.; Frankevich, V.E.; Sukhikh, G.T. Search for New Participants in the Pathogenesis of High-Grade Serous Ovarian Cancer with the Potential to Be Used as Diagnostic Molecules. *Life (Basel, Switzerland)* **2022**, *12*, doi:10.3390/life12122017.
17. He, D.; Wang, X.; Zhang, Y.; Zhao, J.; Han, R.; Dong, Y. DNMT3A/3B overexpression might be correlated with poor patient survival, hypermethylation and low expression of ESR1/PGR in endometrioid carcinoma: an analysis of The Cancer Genome Atlas. *Chin. Med. J. (Engl).* **2019**, *132*, 161–170, doi:10.1097/CM9.0000000000000054.
18. Lindgren, P.; Backstrom, T.; Mahlck, C.-G.; Ridderheim, M.; Cajander, S. Steroid receptors and hormones in relation to cell proliferation and apoptosis in poorly differentiated epithelial ovarian tumors. *Int J Oncol* **2001**, *19*, 31–38, doi:10.3892/ijo.19.1.31.
19. Peluso, J.J.; Liu, X.; Saunders, M.M.; Claffey, K.P.; Phoenix, K. Regulation of ovarian cancer cell viability and sensitivity to cisplatin by progesterone receptor membrane component-1. *J. Clin. Endocrinol. Metab.* **2008**, *93*, 1592–1599, doi:10.1210/jc.2007-2771.
20. Miśkiewicz, J.; Mielczarek-Palacz, A.; Gola, J.M. MicroRNAs as Potential Biomarkers in Gynecological Cancers. *Biomedicines* **2023**, *11*, doi:10.3390/biomedicines11061704.
21. Chen, Q.; Shen, S.; Lv, N.; Tong, J. Role of microRNAs in glycolysis in gynecological tumors (Review). *Int. J. Oncol.* **2023**, *62*, doi:10.3892/ijo.2023.5511.
22. Velle, A.; Pesenti, C.; Grassi, T.; Beltrame, L.; Martini, P.; Jaconi, M.; Agostinis, F.; Calura, E.; Katsaros, D.; Borella, F.; et al. A comprehensive investigation of histotype-specific microRNA and their variants in Stage I epithelial ovarian cancers. *Int. J. cancer* **2023**, *152*, 1989–2001, doi:10.1002/ijc.34408.
23. Yousefi, B.; Sadoughi, F.; Asemi, Z.; Mansournia, M.A.; Hallajzadeh, J. Novel Perspectives for the Diagnosis and Treatment of Gynecological Cancers using Dysregulation of PIWI Protein and PiRNAs as Biomarkers. *Curr. Med. Chem.* **2023**, doi:10.2174/0929867330666230214101837.
24. Sohn, E.J.; Oh, S.-O. P-Element-Induced Wimpy Testis Proteins and P-Element-Induced Wimpy Testis-Interacting RNAs Expression in Ovarian Cancer Stem Cells. *Genet. Test. Mol. Biomarkers* **2023**, *27*, 56–64, doi:10.1089/gtmb.2022.0113.
25. Li, G.; Yi, X.; Du, S.; Gong, L.; Wu, Q.; Cai, J.; Sun, S.; Cao, Y.; Chen, L.; Xu, L.; et al. Tumour-derived exosomal piR-25783 promotes omental metastasis of ovarian carcinoma by inducing the fibroblast to myofibroblast transition. *Oncogene* **2023**, *42*, 421–433, doi:10.1038/s41388-022-02560-y.
26. Das, S.; Majhi, P.D.; Al-Mugotir, M.H.; Rachagani, S.; Sorgen, P.; Batra, S.K. Membrane proximal ectodomain cleavage of MUC16 occurs in the acidifying Golgi/post-Golgi compartments. *Sci. Rep.* **2015**, *5*, 9759, doi:10.1038/srep09759.
27. Carey, P.; Low, E.; Harper, E.; Stack, M.S. Metalloproteinases in Ovarian Cancer. *Int. J. Mol. Sci.* **2021**, *22*, doi:10.3390/ijms22073403.

28. Rao, T.D.; Tian, H.; Ma, X.; Yan, X.; Thapi, S.; Schultz, N.; Rosales, N.; Monette, S.; Wang, A.; Hyman, D.M.; et al. Expression of the Carboxy-Terminal Portion of MUC16/CA125 Induces Transformation and Tumor Invasion. *PLoS One* **2015**, *10*, e0126633, doi:10.1371/journal.pone.0126633.
29. Chen, S.-H.; Hung, W.-C.; Wang, P.; Paul, C.; Konstantopoulos, K. Mesothelin binding to CA125/MUC16 promotes pancreatic cancer cell motility and invasion via MMP-7 activation. *Sci. Rep.* **2013**, *3*, 1870, doi:10.1038/srep01870.
30. Wang, X.; Ramat, A.; Simonelig, M.; Liu, M.-F. Emerging roles and functional mechanisms of PIWI-interacting RNAs. *Nat. Rev. Mol. Cell Biol.* **2023**, *24*, 123–141, doi:10.1038/s41580-022-00528-0.
31. Dai, P.; Wang, X.; Gou, L.-T.; Li, Z.-T.; Wen, Z.; Chen, Z.-G.; Hua, M.-M.; Zhong, A.; Wang, L.; Su, H.; et al. A Translation-Activating Function of MIWI/piRNA during Mouse Spermiogenesis. *Cell* **2019**, *179*, 1566-1581.e16, doi:10.1016/j.cell.2019.11.022.
32. Vias, M.; Morrill Gavarró, L.; Sauer, C.M.; Sanders, D.A.; Piskorz, A.M.; Couturier, D.-L.; Ballereau, S.; Hernando, B.; Schneider, M.P.; Hall, J.; et al. High-grade serous ovarian carcinoma organoids as models of chromosomal instability. *Elife* **2023**, *12*, doi:10.7554/eLife.83867.
33. da Costa, A.A.B.A.; Baiocchi, G. Genomic profiling of platinum-resistant ovarian cancer: The road into druggable targets. *Semin. Cancer Biol.* **2021**, *77*, 29–41, doi:10.1016/j.semcancer.2020.10.016.
34. Zeng, H.; Chen, L.; Zhang, M.; Luo, Y.; Ma, X. Integration of histopathological images and multi-dimensional omics analyses predicts molecular features and prognosis in high-grade serous ovarian cancer. *Gynecol. Oncol.* **2021**, *163*, 171–180, doi:10.1016/j.ygyno.2021.07.015.
35. Su, H.; Jin, Y.; Tao, C.; Yang, H.; Yang, E.; Zhang, W.-G.; Feng, F. Th2 cells infiltrating high-grade serous ovarian cancer: a feature that may account for the poor prognosis. *J. Gynecol. Oncol.* **2023**, *34*, e48, doi:10.3802/jgo.2023.34.e48.
36. Liu, H.; Zhou, L.; Cheng, H.; Wang, S.; Luan, W.; Cai, E.; Ye, X.; Zhu, H.; Cui, H.; Li, Y.; et al. Characterization of candidate factors associated with the metastasis and progression of high-grade serous ovarian cancer. *Chin. Med. J. (Engl).* **2023**, doi:10.1097/CM9.0000000000002328.
37. Timofeeva, A.; Drapkina, Y.; Fedorov, I.; Chagovets, V.; Makarova, N.; Shamina, M.; Kalinina, E.; Sukhikh, G. Small Noncoding RNA Signatures for Determining the Developmental Potential of an Embryo at the Morula Stage. *Int. J. Mol. Sci.* **2020**, *21*, doi:10.3390/ijms21249399.
38. Høgdall, E.V.S.; Christensen, L.; Høgdall, C.K.; Blaakaer, J.; Gayther, S.; Jacobs, I.J.; Christensen, I.J.; Kjaer, S.K. Prognostic value of estrogen receptor and progesterone receptor tumor expression in Danish ovarian cancer patients: from the "MALOVA" ovarian cancer study. *Oncol. Rep.* **2007**, *18*, 1051–1059.
39. Sevelda, P.; Denison, U.; Schemper, M.; Spona, J.; Vavra, N.; Salzer, H. Oestrogen and progesterone receptor content as a prognostic factor in advanced epithelial ovarian carcinoma. *Br. J. Obstet. Gynaecol.* **1990**, *97*, 706–712, doi:10.1111/j.1471-0528.1990.tb16243.x.
40. Fekete, T.; Rásó, E.; Pete, I.; Tegze, B.; Liko, I.; Munkácsy, G.; Sipos, N.; Rigó, J.J.; Györffy, B. Meta-analysis of gene expression profiles associated with histological classification and survival in 829 ovarian cancer samples. *Int. J. cancer* **2012**, *131*, 95–105, doi:10.1002/ijc.26364.
41. Modugno, F. Ovarian Cancer and Polymorphisms in the Androgen and Progesterone Receptor Genes: A HuGE Review. *Am. J. Epidemiol.* **2004**, *159*, 319–335, doi:10.1093/aje/kwh046.
42. Liu, T.; Chen, L.; Sun, X.; Wang, Y.; Li, S.; Yin, X.; Wang, X.; Ding, C.; Li, H.; Di, W. Progesterone receptor PROGINS and +331G/A polymorphisms confer susceptibility to ovarian cancer: a meta-analysis based on 17 studies. *Tumour Biol. J. Int. Soc. Oncodevelopmental Biol. Med.* **2014**, *35*, 2427–2436, doi:10.1007/s13277-013-1322-x.
43. Kanabekova, P.; Al-Awadi, A.M.; Bauyrzhanova, Z.; Tahtouh, T.; Sarray, S.; Almawi, W.Y. Genetic variation in progesterone receptor gene and ovarian cancer risk: A case control study. *Gene* **2022**, *820*, 146288, doi:10.1016/j.gene.2022.146288.
44. Sharma, A.; Sharma, I. In vitro chemo-preventive efficacy of synthetic progestin Norethindrone in human epithelial ovarian cancer. *Med. Oncol.* **2023**, *40*, 195, doi:10.1007/s12032-023-02061-2.
45. Lian, X.-Y.; Zhang, H.; Liu, Q.; Lu, X.; Zhou, P.; He, S.-Q.; Tang, R.-X.; Cui, J. Ovarian cancer-excreted exosomal miR-199a-5p suppresses tumor metastasis by targeting hypoxia-inducible factor-2α in hypoxia microenvironment. *Cancer Commun. (London, England)* 2020, *40*, 380–385.
46. Jiang, Y.; Shi, Y.; Lyu, T.; Liu, H.; Shen, L.; Zhou, T.; Feng, W. Identification and Functional Validation of Differentially Expressed microRNAs in Ascites-Derived Ovarian Cancer Cells Compared with Primary Tumour Tissue. *Cancer Manag. Res.* **2021**, *13*, 6585–6597, doi:10.2147/CMAR.S320834.

47. Pan, X.; Guo, Z.; Chen, Y.; Zheng, S.; Peng, M.; Yang, Y.; Wang, Z. STAT3-Induced lncRNA SNHG17 Exerts Oncogenic Effects on Ovarian Cancer through Regulating CDK6. *Mol. Ther. Nucleic Acids* **2020**, *22*, 38–49, doi:10.1016/j.omtn.2020.08.006.
48. Yiwei, T.; Hua, H.; Hui, G.; Mao, M.; Xiang, L. HOTAIR Interacting with MAPK1 Regulates Ovarian Cancer skov3 Cell Proliferation, Migration, and Invasion. *Med. Sci. Monit. Int. Med. J. Exp. Clin. Res.* **2015**, *21*, 1856–1863, doi:10.12659/MSM.893528.
49. Bieg, D.; Sypniewski, D.; Nowak, E.; Bednarek, I. MiR-424-3p suppresses galectin-3 expression and sensitizes ovarian cancer cells to cisplatin. *Arch. Gynecol. Obstet.* **2019**, *299*, 1077–1087, doi:10.1007/s00404-018-4999-7.
50. Li, T.; Li, Y.; Gan, Y.; Tian, R.; Wu, Q.; Shu, G.; Yin, G. Methylation-mediated repression of MiR-424/503 cluster promotes proliferation and migration of ovarian cancer cells through targeting the hub gene KIF23. *Cell Cycle* **2019**, *18*, 1601–1618, doi:10.1080/15384101.2019.1624112.
51. Huszar, D.; Theoclitou, M.-E.; Skolnik, J.; Herbst, R. Kinesin motor proteins as targets for cancer therapy. *Cancer Metastasis Rev.* **2009**, *28*, 197–208, doi:10.1007/s10555-009-9185-8.
52. Hao, W.; Zhao, H.; Li, Z.; Li, J.; Guo, J.; Chen, Q.; Gao, Y.; Ren, M.; Zhao, X.; Yue, W. Identification of potential markers for differentiating epithelial ovarian cancer from ovarian low malignant potential tumors through integrated bioinformatics analysis. *J. Ovarian Res.* **2021**, *14*, 46, doi:10.1186/s13048-021-00794-0.
53. Li, T.-F.; Zeng, H.-J.; Shan, Z.; Ye, R.-Y.; Cheang, T.-Y.; Zhang, Y.-J.; Lu, S.-H.; Zhang, Q.; Shao, N.; Lin, Y. Overexpression of kinesin superfamily members as prognostic biomarkers of breast cancer. *Cancer Cell Int.* **2020**, *20*, 123, doi:10.1186/s12935-020-01191-1.
54. Kato, T.; Wada, H.; Patel, P.; Hu, H.; Lee, D.; Ujiie, H.; Hirohashi, K.; Nakajima, T.; Sato, M.; Kaji, M.; et al. Overexpression of KIF23 predicts clinical outcome in primary lung cancer patients. *Lung Cancer* **2016**, *92*, 53–61, doi:https://doi.org/10.1016/j.lungcan.2015.11.018.
55. de Lima, A.B.; Silva, L.M.; Gonçales, N.G.; Carvalho, M.R.S.; da Silva Filho, A.L.; da Conceição Braga, L. Three-Dimensional Cellular Arrangement in Epithelial Ovarian Cancer Cell Lines TOV-21G and SKOV-3 is Associated with Apoptosis-Related miRNA Expression Modulation. *Cancer Microenviron. Off. J. Int. Cancer Microenviron. Soc.* **2018**, *11*, 85–92, doi:10.1007/s12307-017-0203-z.
56. Yang, D.; Zhan, M.; Chen, T.; Chen, W.; Zhang, Y.; Xu, S.; Yan, J.; Huang, Q.; Wang, J. miR-125b-5p enhances chemotherapy sensitivity to cisplatin by down-regulating Bcl2 in gallbladder cancer. *Sci. Rep.* **2017**, *7*, 43109, doi:10.1038/srep43109.
57. Cheng, W.-F.; Huang, C.-Y.; Chang, M.-C.; Hu, Y.-H.; Chiang, Y.-C.; Chen, Y.-L.; Hsieh, C.-Y.; Chen, C.-A. High mesothelin correlates with chemoresistance and poor survival in epithelial ovarian carcinoma. *Br. J. Cancer* **2009**, *100*, 1144–1153, doi:10.1038/sj.bjc.6604964.
58. Shen, J.; Sun, X.; Zhou, J. Insights Into the Role of Mesothelin as a Diagnostic and Therapeutic Target in Ovarian Carcinoma. *Front. Oncol.* **2020**, *10*, doi:10.3389/fonc.2020.01263.
59. Santin, A.D.; Vergote, I.; González-Martín, A.; Moore, K.; Oaknin, A.; Romero, I.; Diab, S.; Copeland, L.J.; Monk, B.J.; Coleman, R.L.; et al. Safety and activity of anti-mesothelin antibody-drug conjugate anetumab ravtansine in combination with pegylated-liposomal doxorubicin in platinum-resistant ovarian cancer: multicenter, phase Ib dose escalation and expansion study. *Int. J. Gynecol. cancer Off. J. Int. Gynecol. Cancer Soc.* **2023**, *33*, 562–570, doi:10.1136/ijgc-2022-003927.
60. Zhang, Y.; Lai, X.; Yue, Q.; Cao, F.; Zhang, Y.; Sun, Y.; Tian, J.; Lu, Y.; He, L.; Bai, J.; et al. Bone marrow mesenchymal stem cells-derived exosomal microRNA-16-5p restrains epithelial-mesenchymal transition in breast cancer cells via EPHA1/NF-κB signaling axis. *Genomics* **2022**, *114*, 110341, doi:10.1016/j.ygeno.2022.110341.
61. Cai, K.; Yang, Y.; Guo, Z.-J.; Cai, R.-L.; Hashida, H.; Li, H.-X. Amentoflavone inhibits colorectal cancer epithelial-mesenchymal transition via the miR-16-5p/HMGA2/β-catenin pathway. *Ann. Transl. Med.* **2022**, *10*, 1009, doi:10.21037/atm-22-3035.
62. Bao, C.; Liu, T.; Qian, L.; Xiao, C.; Zhou, X.; Ai, H.; Wang, J.; Fan, W.; Pan, J. Shikonin inhibits migration and invasion of triple-negative breast cancer cells by suppressing epithelial-mesenchymal transition via miR-17-5p/PTEN/Akt pathway. *J. Cancer* **2021**, *12*, 76–88, doi:10.7150/jca.47553.
63. Wang, X.; Wei, P.; Yang, L.; Liu, F.; Tong, X.; Yang, X.; Su, L. MicroRNA-20a-5p regulates the epithelial-mesenchymal transition of human hepatocellular carcinoma by targeting RUNX3. *Chin. Med. J. (Engl).* **2022**, doi:10.1097/CM9.0000000000001975.

64. Shen, E.; Wang, X.; Liu, X.; Lv, M.; Zhang, L.; Zhu, G.; Sun, Z. MicroRNA-93-5p promotes epithelial-mesenchymal transition in gastric cancer by repressing tumor suppressor AHNAK expression. *Cancer Cell Int.* **2020**, *20*, 76, doi:10.1186/s12935-019-1092-7.
65. Wyman, S.K.; Parkin, R.K.; Mitchell, P.S.; Fritz, B.R.; O'Briant, K.; Godwin, A.K.; Urban, N.; Drescher, C.W.; Knudsen, B.S.; Tewari, M. Repertoire of microRNAs in epithelial ovarian cancer as determined by next generation sequencing of small RNA cDNA libraries. *PLoS One* **2009**, *4*, e5311, doi:10.1371/journal.pone.0005311.
66. Nam, E.J.; Yoon, H.; Kim, S.W.; Kim, H.; Kim, Y.T.; Kim, J.H.; Kim, J.W.; Kim, S. MicroRNA expression profiles in serous ovarian carcinoma. *Clin. cancer Res. an Off. J. Am. Assoc. Cancer Res.* **2008**, *14*, 2690–2695, doi:10.1158/1078-0432.CCR-07-1731.
67. Saral, M.A.; Tuncer, S.B.; Odemis, D.A.; Erdogan, O.S.; Erciyas, S.K.; Saip, P.; Ozel, S.; Yazici, H. New biomarkers in peripheral blood of patients with ovarian cancer: high expression levels of miR-16-5p, miR-17-5p, and miR-638. *Arch. Gynecol. Obstet.* **2022**, *305*, 193–201, doi:10.1007/s00404-021-06138-z.
68. Resnick, K.E.; Alder, H.; Hagan, J.P.; Richardson, D.L.; Croce, C.M.; Cohn, D.E. The detection of differentially expressed microRNAs from the serum of ovarian cancer patients using a novel real-time PCR platform. *Gynecol. Oncol.* **2009**, *112*, 55–59, doi:10.1016/j.ygyno.2008.08.036.
69. Gou, L.-T.; Dai, P.; Yang, J.-H.; Xue, Y.; Hu, Y.-P.; Zhou, Y.; Kang, J.-Y.; Wang, X.; Li, H.; Hua, M.-M.; et al. Pachytene piRNAs instruct massive mRNA elimination during late spermiogenesis. *Cell Res.* **2014**, *24*, 680–700, doi:10.1038/cr.2014.41.
70. Goh, W.S.S.; Falciatori, I.; Tam, O.H.; Burgess, R.; Meikar, O.; Kotaja, N.; Hammell, M.; Hannon, G.J. PiRNA-directed cleavage of meiotic transcripts regulates spermatogenesis. *Genes Dev.* **2015**, *29*, 1032–1044, doi:10.1101/gad.260455.115.
71. Zhang, Q.; Zhu, Y.; Cao, X.; Tan, W.; Yu, J.; Lu, Y.; Kang, R.; Wang, X.; Li, E. The epigenetic regulatory mechanism of PIWI/piRNAs in human cancers. *Mol. Cancer* **2023**, *22*, 45, doi:10.1186/s12943-023-01749-3.
72. Sun, Y.H.; Wang, R.H.; Du, K.; Zhu, J.; Zheng, J.; Xie, L.H.; Pereira, A.A.; Zhang, C.; Ricci, E.P.; Li, X.Z. Coupled protein synthesis and ribosome-guided piRNA processing on mRNAs. *Nat. Commun.* **2021**, *12*, 5970, doi:10.1038/s41467-021-26233-8.
73. Nishioka, Y.; Imaizumi, H.; Imada, J.; Katahira, J.; Matsuura, N.; Hieda, M. SUN1 splice variants, SUN1_888, SUN1_785, and predominant SUN1_916, variably function in directional cell migration. *Nucleus* **2016**, *7*, 572–584, doi:10.1080/19491034.2016.1260802.
74. Ching, Y.-P.; Chan, S.-F.; Jeang, K.-T.; Jin, D.-Y. The retroviral oncoprotein Tax targets the coiled-coil centrosomal protein TAX1BP2 to induce centrosome overduplication. *Nat. Cell Biol.* **2006**, *8*, 717–724, doi:10.1038/ncb1432.
75. D'Assoro, A.B.; Lingle, W.L.; Salisbury, J.L. Centrosome amplification and the development of cancer. *Oncogene* **2002**, *21*, 6146–6153, doi:10.1038/sj.onc.1205772.
76. Pancione, M.; Cerulo, L.; Remo, A.; Giordano, G.; Gutierrez-Uzquiza, Á.; Bragado, P.; Porras, A. Centrosome Dynamics and Its Role in Inflammatory Response and Metastatic Process. *Biomolecules* **2021**, *11*, doi:10.3390/biom11050629.
77. LoMastro, G.M.; Holland, A.J. The Emerging Link between Centrosome Aberrations and Metastasis. *Dev. Cell* **2019**, *49*, 325–331, doi:https://doi.org/10.1016/j.devcel.2019.04.002.
78. van Driel, W.J.; Koole, S.N.; Sikorska, K.; Schagen van Leeuwen, J.H.; Schreuder, H.W.R.; Hermans, R.H.M.; de Hingh, I.H.J.T.; van der Velden, J.; Arts, H.J.; Massuger, L.F.A.G.; et al. Hyperthermic Intraperitoneal Chemotherapy in Ovarian Cancer. *N. Engl. J. Med.* **2018**, *378*, 230–240, doi:10.1056/NEJMoa1708618.
79. Langmead, B.; Trapnell, C.; Pop, M.; Salzberg, S.L. Ultrafast and memory-efficient alignment of short DNA sequences to the human genome. **2009**, *10*, doi:10.1186/gb-2009-10-3-r25.
80. Team, R.C. A language and environment for statistical computing. R Foundation for Statistical Computing, Vienna, Austria Available online: https://www.r-project.org (accessed on Mar 10, 2021).
81. Love, M.I.; Huber, W.; Anders, S. Moderated estimation of fold change and dispersion for RNA-seq data with DESeq2. **2014**, 1–21, doi:10.1186/s13059-014-0550-8.
82. Daltoé, R.D.; Madeira, K.P.; de Carvalho, A.A.; de Rezende, L.C.D.; Silva, I.V.; Rangel, L.B.A. Evaluation of the progesterone receptor status in breast cancer using three different antibodies: a comparison by Allred score system. *Int. J. Clin. Exp. Pathol.* **2014**, *7*, 331–339.
83. Team, Rs. RStudio: Integrated Development for R. RStudio Available online: http://www.rstudio.com/. (accessed on Mar 23, 2021).

 doi:10.20944/preprints202307.1155.v1